MASTERARBEIT | MASTER‘S THESIS

Titel | Title

Effects of micro- and nanoplastic particles in an $APC^{Min/+}$ intestinal neoplasia model

verfasst von | submitted by

Saulė Bertalytė BSc

angestrebter akademischer Grad | in partial fulfilment of the requirements for the degree of

Magistra pharmaciae (Mag. pharm.)

Wien | Vienna, 2026

Studienkennzahl lt. Studienblatt | Degree programme code as it appears on the student record sheet:	UA 066 605
Studienrichtung lt. Studienblatt | Degree programme as it appears on the student record sheet:	Masterstudium Pharmazie
Betreut von | Supervisor:	Assoz. Prof. Mag. Dr. Verena Pichler

Acknowledgment

First and foremost, I would like to thank Dr. Verena Kopatz for the given opportunity to be a part of her research project and gain valuable experience while working on *in vivo* mouse experiments. Her continuous guidance, support and mentorship have contributed greatly to the successful completion of my master´s thesis.

In addition, I would also like to thank Univ.-Prof. Dr. Lukas Kenner for the opportunity to work at his laboratory and be a part of the microONE project. During this period of my master's degree, I gained meaningful insight into the routine and practice of scientific research and had the privilege to work with wonderful and brilliant people.

I would especially like to express my gratitude to Assoc. Prof. Mag. Dr. Verena Pichler for her supervision and invaluable academic mentorship. Her unwavering support in navigating the formal procedures towards the completion of my thesis greatly eased this challenging period.

Finally, I am exceptionally grateful to my family and friends who supported and motivated me throughout the studies and the writing of my thesis.

Abstract

Colorectal cancer (CRC) is one of the most prevalent cancer types in modern society. Familial adenomatous polyposis (FAP) is a hereditary genetic disorder and a risk factor for CRC in humans. FAP is caused by a genetic nonsense mutation in the adenomatous polyposis coli (APC) tumour suppressor gene which leads to increased intestinal adenoma development. The same APC gene mutation in mice also leads to multiple intestinal polyp formation, mainly in the small intestine.

Plastic is one of the main environmental pollutants of the last century. An even more pressing topic are micro- and nanoplastic (MNP) particles. The environmental and health effects of these particles are still widely unknown; however, it has been shown, that they can cause intestinal barrier disruption, oxidative stress and inflammation. The main route of MNP exposure is ingestion, which makes the gastrointestinal tract the main destination of possible damaging effect and particle accumulation. For this reason, we wanted to investigate the effect of MNPs on intestinal tumour progression, as well as physiological and immunological changes.

Two long-term experiments – 100-day and survival - were conducted on an $APC^{Min/+}$ mouse model. One groups of mice received polystyrene (PS) MNP-supplemented mouse food while the control (Ctr) group received normal mouse food (0.3 mg PS-mix/g food). After reaching experimental endpoint, organs were sampled and histopathological evaluation of the small intestine was performed.

MNP-treated mice displayed a significantly lower average polyp area and spleen weight. Also, the overall survival of MNP-treated $APC^{Min/+}$ mice was slightly reduced compared to Ctr mice. This might indicate, that despite lower polyp burden, the overall survival was still decreased with MNP treatment, which could point toward other pathological pathways of MNPs - such as inflammation - which could influence overall survival in this model aside from tumour promoting effects. In summary, it was found, that MNPs have an effect on tumour development and less so on overall survival. Although the two parameters display no direct correlation, there is most likely an indirect effect, mediated by inflammatory processes. More research needs to be conducted in order to thoroughly investigate the involved molecular mechanisms.

Zusammenfassung

Darmkrebs (CRC) ist eine der häufigsten Krebsarten in der heutigen Gesellschaft. Die familiäre adenomatöse Polyposis (FAP) ist eine vererbbare genetische Erkrankung und ein Risikofaktor für Darmkrebs beim Menschen. FAP wird durch eine genetische Nonsense-Mutation im Tumorsuppressorgen „Adenomatous Polyposis Coli" (APC) verursacht, die zu einer vermehrten Bildung von Darmadenomen führt. Die gleiche APC-Genmutation führt auch bei Mäusen zur Bildung zahlreicher Darmpolypen, vor allem im Dünndarm.

Kunststoff ist einer der größten Umweltverschmutzer, wobei Mikro- und Nanoplastikpartikel (MNP) dadurch ein dringliches Thema geworden sind, deren Auswirkungen auf Umwelt und Gesundheit noch weitgehend unbekannt sind. Es wurde gezeigt, dass sie eine Störung der Darmbarriere, oxidativen Stress und Entzündungen verursachen können. Der Hauptexpositionsweg ist die orale Aufnahme, wodurch der Magen-Darm-Trakt zum Ziel möglicher negativer Auswirkung sowie einer Anreicherung wird. Das Ziel der Arbeit war es die möglichen Auswirkungen von MNPs auf das Fortschreiten von Darmtumoren sowie die physiologischen und immunologischen Veränderungen zu untersuchen.

Zwei Langzeitversuche – ein 100-Tage und ein Überlebensversuch – wurden an einem $APC^{Min/+}$-Mausmodell durchgeführt, wobei eine Gruppe Futter mit Polystyrol (PS)-MNP (0.3 mg PS-mix/g Futter) erhielt. Überlebenszeit und histopathologische Veränderungen wurden im Dünndarm untersucht.

MNP-behandelte Mäuse wiesen signifikant kleinere Polypen und ein geringeres Milzgewicht auf. Auch die Gesamtüberlebenszeit der MNP-behandelten $APC^{Min/+}$-Mäuse war im Vergleich zu den Control(Ctr)-Mäusen leicht verkürzt. Da die Gesamtüberlebenszeit trotz geringerer Polypenbelastung bei MNP-Exposition immer noch niedriger war, könnte das darauf hindeuten, dass es zusätzlich zu den beschriebenen Effekten auf das Polypenwachstum noch andere pathologische Wirkmechanismen der MNPs in diesem Kontext gibt, wie beispielsweise Verstärkung von Entzündungen. Schlussendlich, es wurde gezeigt, dass MNPs einen Einfluss auf die Tumorentwicklung haben und etwas weniger auf Gesamtüberleben. Obwohl zwischen den beiden Parametern kein direkter Zusammenhang besteht, ein indirekter Effekt wird vermutet, der durch Entzündungsprozesse vermittelt wird. Es sind also weitere Untersuchungen erforderlich, um die beteiligten molekularen Mechanismen gründlich zu erforschen.

Table of Contents

1. Introduction

1.1. Biological and clinical relevance of intestinal neoplasia

1.1.1. Epidemiology, predisposition and clinical significance

Among rising cancer incidents, colorectal cancer (CRC) represents a major health burden in modern society. GLOBOCAN-based estimates from the year 2022 reported approximately 1.93 million new CRC cases and 904 019 CRC-related deaths worldwide (Wu et al., 2025). Males exhibited an almost 1.5 times higher CRC incident and mortality risk compared to females. Most record values documented in Europe underlined a positive correlation between HDI (human development index) and CRC-cases being shown in general (Wu et al., 2025). Although the highest prevalence for CRC is still over the age of 65, in some regions increasing rates among younger adults have been reported, highlighting the need to investigate possible lifestyle-related and environmental risk factors (Siegel et al., 2026).

In a study conducted on twins in northern Europe, it has been estimated that approximately 35% of CRC susceptibility is related to genetic factors, while environmental influences still remain the central cause for most sporadic cases (Lichtenstein et al., 2000). Hereditary syndromes, such as Lynch syndrome and familial adenomatous polyposis (FAP), contribute to intestinal cancer risk with one-third of CRC cases displaying an inherited or familial component (Jasperson et al., 2010). However, most CRC cases occur sporadically and are influenced by modifiable factors, including nutrition, physical activity, alcohol consumption, and smoking (Keum & Giovannucci, 2019). Intestinal tumorigenesis is therefore best understood as the resulting combination of both genetic predisposition and environmental or lifestyle-related influences.

In contrast to CRC, small intestine neoplasia, despite its extensive mucosal surface, is comparably rare. Even so, the incidence rate appears to have increased throughout the years with adenocarcinomas representing one of the major histological subtypes, constituting for around 37% of small bowel malignancies, followed by neuroendocrine tumours (34%), lymphomas (14%) and sarcomas (12%) (Bouvier et al., 2019). The highest cancer frequency

was located in duodenum with a comparatively lower load in ileum and jejunum (Legué et al., 2016). Despite shared molecular features with CRC, including alterations in Kirsten rat sarcoma virus oncogene homologue (KRAS), tumour protein 53 (TP53), adenomatous polyposis coli (APC) genes and mismatch-repair pathways, varying mutations frequencies in small intestine tumorigenesis and a more common association with predisposing diseases indicate a partly diverse carcinogenic as compared to CRC (Aparicio et al., 2022a).

These findings highlight the clinical relevance of intestinal neoplasia and support experimental investigation of factors, that may influence intestinal tumour development as well as tissue morphology, inflammation and disease progression.

1.1.2. Stages of tumorigenesis

Of the several pathways, that are responsible for gastrointestinal tumorigenesis, adenoma to carcinoma sequence is the most common one. A gradual accumulation of genetic modifications results in the conversion of normal cells to an adenoma, which eventually develops into a malignant tumour (Keum & Giovannucci, 2019). Despite the length and mucosal surface area of the small intestine, cancer formation here is comparatively rare. The contradiction is most probably a result of protective features of the local environment, such as rapid transit and dilution of luminal contents, lower bacterial density, distinct bile-acid metabolism and slightly alkaline pH-levels at distal ileum (Aparicio et al., 2022).

The early stage of intestinal carcinogenesis is believed to involve transformation of normal mucosa into adenomatous precursor lesions through incorrect regulation / mutation in various pathways. Tumour initiation may occur randomly through molecular alterations or be promoted by predisposing conditions including Crohn's disease, coeliac disease, Lynch syndrome and FAP, which increase epithelial damage, inflammatory signalling and genomic instability (Figure 1) (Aparicio et al., 2014; Nguyen et al., 2020; Schottenfeld et al., 2009).

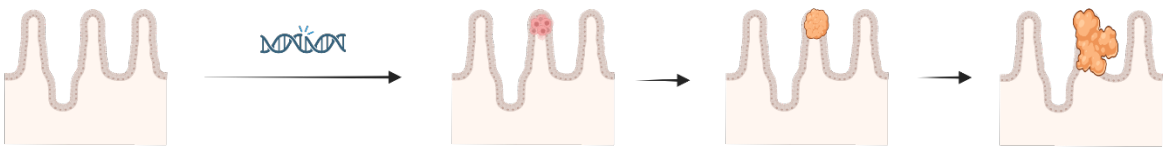

Figure 1: Schematic illustration of tumorigenesis in gastrointestinal tissue. Initiated mainly through genetic predisposition e.g. APC-inactivation or BRAF transformation to oncogene) or random inflammation-induced genetic mutations. These mutations lead to an uncontrolled epithelial cell proliferation, followed by increasingly abnormal tissue morpholgy and eventually to a potentially invasive character. Created with BioRender.com

At the molecular level, small bowel adenocarcinomas are highly similar to CRC, however, it has been shown, that there´s a significant difference in the frequency of prevalent genetic alterations between these cancer types (Schrock et al., 2017). The most common genetic mutations in small intestine neoplasia include *KRAS*, *TP53*, suppressor of mothers against decapentaplegic homologs (*SMAD4)*, *APC*, Phosphatidylinositol-4,5-bisphosphate 3-kinase catalytic subunit alpha (*PIK3CA)*, B-Raf proto-oncogene - serine/threonine kinase *(BRAF)*, erythroblastic oncogene B/ human epidermal growth factor receptor 2 *(ERBB2/HER2)* (Schrock et al., 2017). As tumorigenesis progresses, additional mechanisms, such as epigenetic variations, mismatch-repair impairment and alterations in cellular signalling pathways increasingly contribute to a malignant shift (Schottenfeld et al., 2009).

To put it briefly, small intestine neoplasia is initiated through either epithelial injury, hereditary predisposition or random molecular alterations. Further development involves dysplasia, adenomatous growth, and inflammatory signalling (Aparicio et al., 2022b; Schottenfeld et al., 2009), whereas additional progression is driven by genomic and epigenomic abnormalities (Schrock et al., 2017).

1.1.3. APC mutation and dysregulation of Wnt/β-catenin signalling.

Mutations in the APC gene are considered to be one of the major early events in colorectal carcinogenesis (Ren et al., 2019). A loss-of-function mutation can lead to a lack of cell adhesion, wingless-related integration site (Wnt)-pathway activation, impairment in cell cycle control, dysfunctional DNA-repair mechanisms and spindle dysfunction (L. Zhang & Shay, 2017). Normally, the APC protein is a part of a destruction complex directed at β-catenin, which is a key signal transductor for the Wnt-pathway. It causes inhibition of β-catenin/ T-cell factor (TCF)-4 signalling, which in turn induces G1 cell-cycle arrest and promotes intestinal differentiation (Van de Wetering et al., 2002).

Colon carcinoma cells, that exhibit an absent APC tumour suppressor protein, contain a stable nuclear β-catenin–hTCF-4 complex, resulting in continuous transcriptional activation of TCF target genes via the Wnt-pathway. Reintroduction of wild-type APC disrupted this β-catenin–TCF transcriptional activity, supporting the concept that APC normally functions as a negative regulator of β-catenin signalling (Korinek et al., 1997). Comparable effects are expected in small intestine due to the similar genetic profile with colon (Schottenfeld et al., 2009). Conclusively, APC mutation promotes intestinal neoplasia by allowing β-catenin to accumulate, enter the nucleus and activate transcriptional programmes that contribute to epithelial transformation.

A study done by Barker et al. found, that a selective deletion of APC-gene in highly proliferative leucine-rich repeat-containing G-protein coupled receptor 5 (Lgr5)-positive intestinal stem cells caused β-catenin to accumulate within days and induce progressively growing microadenomas, that developed into macroscopic adenomas within weeks. In contrast, APC deletion in short-lived progenitor cells generated lesions whose growth rapidly stalled, indicating that the cellular context of APC mutation is crucial. This supports the concept that Wnt/β-catenin activation has the strongest cancerogenic effect when it occurs in self-renewing intestinal stem cells, which can sustain neoplastic growth (Barker et al., 2008b). Consequently, unrestricted Wnt-pathway activation causes rapid disruption of epithelial homeostasis, such as increased proliferation, inadequate differentiation, abnormal Paneth cell positioning and defective cell migration (Sansom et al., 2004). APC is a key regulator of intestinal cell fate, not only by restraining β-catenin transcriptional activity, but also by maintaining normal crypt architecture, epithelial movement and differentiation.

Additionally, Fre et al. found, that Wnt/TCF4 signalling positively affects Notch-driven cancer cell proliferation. In mice, that carry an unfunctional APC protein, activation of Notch markedly increased adenoma formation, shortened tumour latency and produced proliferative lesions with nuclear β-catenin, indicating active Wnt signalling. Therefore, APC mutation and β-catenin activation provide a permissive oncogenic state, but additional epithelial signalling pathways such as Notch can intensify proliferation and tumour initiation (Fre et al., 2009).

Collectively, these studies show that APC mutation is a central initiating event in intestinal neoplasia because it prevents β-catenin degradation, causing constitutive β-catenin/TCF transcriptional activity and maintenance of a proliferative carcinogenic state.

1.1.4. Inflammatory characteristics of intestinal tumour development

Intestinal inflammations trigger additional routes of intestinal tumour formation. In colitis-associated cancer, chronic mucosal injury, due to inflammation and repeated repair cycles, can drive epithelial transformation to progress to dysplasia and finally carcinoma (Terzić et al., 2010). Molecular abnormalities, such as chromosomal instability, microsatellite instability and DNA hypermethylation may already be detectable in inflamed and injured mucosa before histological dysplasia appears, suggesting that inflammation creates a field of genetically and epigenetically modified epithelium that is predisposed to malignant progression (Itzkowitz & Yio, 2004).

Activated immune cells - macrophages, dendritic cells, neutrophils and T-cell subgroups - release reactive oxygen and nitrogen species that can induce DNA damage, mutations and epigenetic silencing of tumour-suppressor genes. At the same time, pro-inflammatory cytokines such as tumour necrose factor (TNF), interleukin (IL)-6, IL-1, IL-17 and IL-23 activate key transcription factors, particularly NF-κB, STAT3, PI3K/AKT and Wnt/β-catenin, which promote epithelial resistance to apoptosis, clonal expansion of premalignant cells, angiogenesis and tumour progression (Grivennikov, 2013; Terzić et al., 2010).

Moreover, inflammation can induce epigenetic changes, such as DNA methylation and microRNA-mediated silencing of tumour-suppressor and DNA-repair genes (Terzić et al., 2010). Intestinal microbiota further regulates this process by influencing mucosal immune activation, epithelial proliferation and cytokine production (Grivennikov, 2013; Terzić et al., 2010). In addition, it has been determined that the severity of inflammation itself is a decisive factor especially for colorectal neoplasia risk. In a case-control study of patients with long-standing extensive ulcerative colitis, both colonoscopic and histological inflammation scores were associated with colorectal neoplasia, with the latter being the strongest predictor (Rutter et al., 2004).

Chronic intestinal inflammation promotes tumour development by creating a pro-mutagenic and growth-supportive microenvironment characterized by epithelial injury,

repeated regeneration, oxidative DNA damage, cytokine signalling, immune-cell infiltration, microbiota-driven activation, and activation of key oncogenic molecular pathways. Together, these mechanisms support the tumorigenesis progression making the severity and persistence of inflammation key determinants of intestinal neoplasia risk.

1.1.5. Characteristics of the $APC^{Min/+}$ genetic mouse model

The $APC^{Min/+}$ mouse model is a widely used genetic model of intestinal neoplasia. Due to a nonsense point mutation in the murine APC gene, at codon 850, spontaneous adenomas in the small intestine start to form (Moser et al., 1995). Conveniently, this mutation highly resembles the human FAP condition, which is also a result of a gremline APC mutation. This makes the model especially useful for studying early-stage APC-driven tumour formation, cancer variety, genetic modifier effects and the influence of local intestinal factors on adenoma development (Moser et al., 1995).

$APC^{Min/+}$ mice are used only as heterozygous carriers (mutant males bred with C57BL/6 wildtype females) of the APC mutation, because homozygous subjects don´t survive. Around four months of age mutant mice develop mostly small intestinal adenomas, with fewer colonic lesions (Boivin et al., 2003). It has also been noted by Moser et al., that intestinal tumour number strongly depends on the genetic background, with resistant strains showing markedly fewer tumours. In addition, it has been reported that tumours commonly show loss of the wild-type APC allele, supporting the role of the gene loss as a central event in adenoma formation (Moser et al., 1995). Most formations are benign, although progression to invasive adenocarcinoma happens occasionally. The main pathological features of $APC^{Min/+}$ intestinal tumours are, that they usually arise without inflammation, often protrude into the intestinal lumen and resemble human adenomas microscopically (Boivin et al., 2003). Thus, it makes the genetic mutant mouse model most suitable for studying early adenoma induction and progression.

Tumour development in the $APC^{Min/+}$ mice is determined not only by the APC mutation itself, but is also influenced by the animal's genetic background. A study done by Dietrich et al. identified Mom1, a crucial modifier locus on distal chromosome 4, which is largely responsible for variations in the number of intestinal polyps between mouse strains. This finding is important, as it describes the mutant mouse model as genetically sensitive, where tumour burden can change depending on inherited modifier genes (Dietrich et al., 1993).

In conclusion, due to physiological properties of the $APC^{Min/+}$ mouse model, it is best used for studying effects connected to early intestinal tumour formation and modifier mechanisms.

1.2. Micro- and nanoplastic (MNP) pollution

1.2.1. Global consequences of plastic pollution

Plastic pollution has been one of the main hot topics globally for more than half a century. Its implementation in packaging, construction, textile, consumer products, transportation and industry has significantly increased over the years (Geyer et al., 2017). This has unfortunately led to an unmanageable escalation in plastic pollution worldwide. In the year 2025 the Plastic Overshoot Day was reached on the 5th of September (Perreard, 2025). This marks the day of the year when accumulated plastic waste globally exceeds the capacity to recycle it, thus leading to environmental pollution. Combined with its widespread use in daily life, plastic´s resistance to degradation has made it to one of modern societies biggest environmental problems. Even though about 12% of urban waste is credited to plastic (Fayshal, 2024), a much larger proportion of debris, found floating on the ocean surface, on the shoreline and deposited on the seabed is made of plastic. Plastic waste can be found all over - in urban areas, remote islands, water bodies and even polar regions (Barnes et al., 2009). Its persistence is estimated to range from decades to hundreds of years and may be even longer in cold and dark environments, such as deep-sea floors (MacLeod et al., 2021). Plastic half-life depends mainly on its chemical and physical properties and surrounding environmental conditions (Chamas et al., 2020).

Apart from direct environmental problems, plastic is also dangerous to wildlife. Barnes et al. described how macroplastic debris can entangle or choke wildlife, while smaller fragments may enter food chains through ingestion by marine and freshwater organisms. Plastics can also act as vectors for non-native species, allowing organisms to attach to floating debris and disperse across large distances (Barnes et al., 2009). This shows that plastic pollution is not only an aesthetic or waste-management issue, but also a biological and ecological problem with consequences for the environment, biodiversity and ecosystem stability.

1.2.2. Formation, classification and properties of MNPs

As plastic materials accumulate in terrestrial, freshwater and marine environments, they undergo subsequent fragmentation into smaller particles (Barnes et al., 2009). This process links global plastic overproduction and mismanagement directly to MNP pollution, as larger plastic debris continuously break down into smaller fragments, that can persist, disperse and interact with organisms and environmental contaminants more easily (Walker & Fequet, 2023).

Microplastics are generally referred to as plastic particles smaller than 5 mm, whereas nanoplastics are commonly described as particles below 1 μm (Kim et al., 2020). Additionally, larger plastic particles are also described as mesoplastics, which vary between 5 to 25 mm, and macroplastics, which are larger than 25 mm (Kim et al., 2020). This size-based classification is important, because particle detection, bioavailability, toxicity and environmental mobility are substantially influenced by their size (Mariano et al., 2021; Sharma et al., 2022). Smaller particles generally have a higher surface-area-to-volume ratio, greater reactivity and a higher probability of crossing biological barriers, which makes nanoplastics particularly more concerning, compared to larger microplastic particles (Sharma et al., 2022).

Additionally, plastic particles can be divided into primary and secondary particles according to their origin (Mariano et al., 2021). Primary microplastics are intentionally manufactured at microscopic size and used in products, such as cosmetics, personal care products, detergents, pharmaceuticals, paints, insecticides and industrial abrasives (Mariano et al., 2021; Osman et al., 2023). On the other hand, secondary MNPs are formed unintentionally, through the biological or mechanical fragmentation and degradation of larger plastic items, including household items, products from industrial manufacture, debris from disposed car tires and more (Mariano et al., 2021). Secondary microplastics are considered especially difficult to control because they are continuously being generated from already existing plastic waste in the environment (Osman et al., 2023).

The formation of secondary MNPs is driven by several physical, chemical and biological degradation processes. Environmental exposure to UV-radiation, mechanical abrasion through e.g. wave action, temperature fluctuations, oxidation, hydrolysis and biological activity weakens plastic materials and promotes cracking, embrittlement and

fragmentation (Chamas et al., 2020). During this degradation process, the physical and chemical properties of the particles change, including surface charge, crystallinity, polarity, roughness and reactivity (Sharma et al., 2022). These changes influence how particles move through water, air, soil and sediments, as well as how they interact with organisms, biofilms, natural organic matter and pollutants (Sharma et al., 2022). As plastic fragments into MNP particles, chemicals present in the plastic material, such as additives, residual monomers and oligomers, as well as degradation products of the polymer itself are released into surrounding area (MacLeod et al., 2021). Additionally, once exposed to the environment a biofilm, consisting of organic matter and microorganisms, can form around plastic particles, which, on one hand, provides an additional sorption phase for chemical substances and, on the other, protects them from e.g. UV-radiation and increases persistence (MacLeod et al., 2021).

Furthermore, MNPs may also be classified according to shape, such as fragments, fibres, films, foams, pellets (Osman et al., 2023). This classification is relevant because particle shape affects transport, ingestion and biological interaction (Mariano et al., 2021). For example, fibres released from synthetic textiles may behave differently in the surrounding environment than irregular fragments formed from broken packaging, whereas films and foams may have different buoyancy and fragmentation behaviour. Certain microplastic shapes, especially cylindrical and elongated shapes, result in longer suspension times in bodies of water due to drag forces and irregular fluctuations (MacLeod et al., 2021).

MNPs can also be classified according to polymer composition, with common types including polyethylene, polypropylene, polystyrene (PS), polyvinyl chloride, polyethylene terephthalate, polyurethane, nylon and cellulose acetate (Mariano et al., 2021; Osman et al., 2023). Polymer type influences density, degradation rate, buoyancy, chemical stability and affinity for environmental contaminants.

Nanoplastics are considered potentially more hazardous than microplastics due to their smaller size, which gives them greater mobility, abundance and biological accessibility (Sharma et al., 2022). Due to their dimensions, nanoplastics may remain suspended in environmental media for longer periods, travel further from their source and interact more strongly with cells and biomolecules (MacLeod et al., 2021; Sharma et al., 2022). Additionally, nanoplastic particle reactivity and ability to bind or release chemical

substances is elevated, as a result of their surface area-to-volume ratio (Sharma et al., 2022). Moreover, nanoplastics might have the ability to penetrate biological membranes more easily than larger microplastics, raising concerns about cellular uptake, tissue translocation and toxicological effects that are still not fully understood (MacLeod et al., 2021; Sharma et al., 2022).

One of the major scientific challenges regarding MNPs is that they are difficult to identify and quantify accurately. Given that microscopical identification of these particles is generally insufficient, physical characterization is usually combined with chemical analysis methods, such as infrared spectroscopy, Raman spectroscopy, mass spectrometry or elemental analysis to determine the polymer type (Mariano et al., 2021). Nanoplastics are even more difficult to study, as the resolution needed to detect them is often below that of conventional optical microscopy, in which case weak analytical signals are produced (Mariano et al., 2021). Advanced techniques, such as scanning electron microscopy, transmission electron microscopy, atomic force microscopy, dynamic light scattering and Raman imaging are implemented more often, however standardization of these methods remains limited (Mariano et al., 2021).

Overall, MNPs represent a heterogeneous group of environmental particles, existing mainly as a result of general plastic waste degradation and partly due to direct release of intentionally manufactured MNPs. They are classified based on size, origin, shape and chemical composition, while their environmental behaviour is determined by physicochemical properties, such as density, chemical composition, polymer type, degradation state and interaction with surrounding material. Understanding these properties is crucial for the accurate assessment of potential biological and environmental dangers.

1.2.3. Main routes of plastic uptake into the human body

Nowadays, MNPs can be detected in food, drinking water, air and dust. This continuous exposure can result from both environmental contamination and as a consequence of direct daily contact with plastic-containing products (Dick Vethaak & Legler, 2021). Ingestion and inhalation are regarded to be the main routes of MNP-uptake in humans, whereas dermal uptake is considered less relevant, provided that the skin barrier is not damaged (Leslie et al., 2022). The biological relevance for human health relies not only on the quantity of

particles entering the body, but also on their physicochemical properties and whether particles can cross biological barriers. (Dick Vethaak & Legler, 2021).

As previously established, the main route of plastic uptake in humans is oral ingestion. MNPs were shown to enter the gastrointestinal tract through contaminated food and beverages, such as seafood, salt, sugar, honey, alcohol and bottled water (Cox et al., 2019). A review, done by Cox et al. and covering 26 various scientific studies, estimated that the annual intake of microplastic through ingestion was around 39,000–52,000 particles per person, depending on age and sex. When inhalation was also included, estimations increased to 74,000–121,000 particles per year. Different sources of drinking-water were considered as an especially important parameter: individuals consuming only bottled water were estimated to ingest an additional 90,000 particles per year, compared to ~ 4000 particles for those consuming only tap water (Cox et al., 2019).

Following ingestion, most of the larger plastic particles are expected to remain within the gastrointestinal lumen and eventually get eliminated with faeces. However, there is a possibility, that smaller particles might interact more closely with the intestinal mucosa and, to a limited extent, cross the gut barrier (Dick Vethaak & Legler, 2021; Stock et al., 2019). This is particularly relevant with regard to small intestine, as it is the main absorptive organ of the gastrointestinal tract and contains specialized epithelial structures involved in nutrient uptake. Small bowel cells possess different functions: enterocytes form a tight epithelial barrier, goblet cells produce a protective mucus layer and microfold cells can transport particles from the intestinal lumen toward mucosa-associated lymphoid tissue, such as Peyer's patches (Stock et al., 2019). According to the reviewed evidence, only a very small fraction of particles, below ~ 150 μm, may cross the intestinal mucus barrier, while transport to deeper tissues is expected only for much smaller particles, below ~ 1.5 μm (Stock et al., 2019).

Another important uptake route is inhalation of airborne MNPs and fibres. Airborne particles may originate from synthetic textiles, tire wear, household dust, furniture, building materials, traffic, waste incineration, landfills and industrial emissions (Prata, 2018). It is suggested, that indoor exposure may be particularly relevant, because humans spend a large proportion of time indoors, where proper ventilation might be limited, and exposure to daily sources of MNPs, like synthetic textiles and indoor dust might be more

concentrated. Indoor concentrations were reported ranging from 0.4 to 59.5 particles/m^3, with a substantial fraction containing polymers (Dris et al., 2017). Inhaled microplastics may remain in the respiratory tract and cause irritation or inflammation, be cleared by mucociliary transport and swallowed or potentially cross the lung epithelium if sufficiently small (Dick Vethaak & Legler, 2021; Prata, 2018). This indicates that inhalation can contribute both to respiratory exposure and indirectly to gastrointestinal exposure (Cox et al., 2019). It has been noted that larger particles, settled in the respiratory tract, are likely cleared toward the gut, while smaller particles may pose more biologically relevant threat, because uptake efficiency generally increases as particle size decreases (Dick Vethaak & Legler, 2021). Evidence from cell and animal studies suggests, that particles below 10 μm, after they have reached the gut, can translocate from the gut cavity into lymphatic and circulatory systems, while nanoscale particles below 0,1 μm may have the potential to cross cell membranes and reach organs. Despite the existing data, absorption, distribution, metabolism and excretion of plastic particles in humans remains largely unexplored (Dick Vethaak & Legler, 2021).

Evidence of human exposure and systemic uptake of MNPs is provided by the detection of plastic particles in human blood. In a study performed by (Leslie et al., 2022), where blood of 22 healthy volunteers was analysed, several polymers were detected, with polyethylene terephthalate, polyethylene and styrene-based polymers being the most frequently encountered. The average concentration of plastic particles in blood was 1.6 μg/ml, providing the first measurement of polymer mass concentration in human blood and demonstrating that at least some plastic particles are bioavailable for uptake into the bloodstream (Leslie et al., 2022). Blood is considered as a transport compartment that can distribute particles further throughout the body, but whether particles are rapidly eliminated or accumulate in organs remains unclear (Leslie et al., 2022).

To sum up, evidence shows that humans are exposed to MNPs through food, drinking water and air and that a fraction of these particles can enter the body internally. Ingestion and inhalation are the dominant uptake routes, with gastrointestinal and respiratory barriers acting as the main uptake interfaces for environmental plastic particles. While most larger particles are probably excreted or cleared, smaller microplastics and nanoplastics may cross epithelial barriers and reach systemic circulation.

1.3. Biological effects of MNP in the gastrointestinal tract

1.3.1. Health risks posed by MNP exposure

As previously described, the main routes of MNP uptake are ingestion and inhalation. Although possible health effects of plastic uptake are not yet fully determined, several mechanisms are considered biologically plausible(Dick Vethaak & Legler, 2021). As previously mentioned, MNP toxicity may occur, if inhaled or ingested particles accumulate locally and trigger immune activation, inflammation or oxidative stress (Dick Vethaak & Legler, 2021; Wright & Kelly, 2017). In the lung, particles, smaller than approximately 2.5 μm, and fibres are considered especially concerning, because they may settle in deeper compartments and be difficult to clear (Wright & Kelly, 2017). Chemical toxicity might also result from leaching of residual monomers, additives or adsorbed pollutants, while microbial toxicity may occur as well, if plastic surfaces carry biofilms of pathogenic bacteria. MNPs may cause physical harm, such as epithelial irritation, oxidative stress, inflammation, cytokine release and cellular damage (Dick Vethaak & Legler, 2021). On the other hand, it has been highlighted, that many toxicological studies use rather high exposure concentrations and pristine commercial particles, that do not fully represent real environmental plastics, making direct translation to human risk difficult (Dick Vethaak & Legler, 2021).

The main uncertainty, regarding MNPs, is not whether exposure is possible, but how much exposure occurs and if it is sufficient to cause disease or any harm to tissues. It has been argued, that chronic exposure is likely more relevant, than acute exposure, because small particles may accumulate and exert quantity-dependent effects over time (Smith et al., 2018). Nanoplastics especially may be of particular concern, because a single microplastic particle can theoretically fragment into a larger number of nanoplastic particles, and these smaller particles may more easily cross biological barrier (Yee et al., 2021) . Due to this, nanoplastics are considered potentially more hazardous, as they may interact with proteins, lipids, carbohydrates and nucleic acids and form biological coronas (Yee et al., 2021). However, current exposure estimates are still incomplete, because analytical methods struggle to detect the smallest particles, especially nanoplastics (Dick Vethaak & Legler, 2021).

In order to better investigate possible health risks of MNPs on living organisms, studies on mice and human cells have been conducted. Experimental research done in mice suggested several possible toxic effects of PS particles, such as gut microbiota alterations, intestinal barrier disruption, oxidative stress, liver inflammation, lipid metabolism disturbance and energy metabolism changes (Yong et al., 2020). Plastic particles were shown to accumulate in the gut, liver and kidney and were associated with inflammatory changes, lipid accumulation, reduced ATP levels and altered hepatic metabolism (Yee et al., 2021). However not all animal studies reported such effects, but some describing also an absence of notable changes lesions or inflammation (Stock et al., 2019). Thus, indicating that MNP effects might not account for all particle types in general, but could be related to specific particle property. In an *in vivo* study by Zhang et al. adult male C57BL/6J mice were exposed for 8 consecutive weeks by oral gavage to either 0.5 μm or 5 μm plastic particles, at 0.5 mg per mouse per day. Afterwards, biodistribution, organ pathology, inflammatory markers, gut microbiota composition and faecal metabolites were assessed. The main finding of this study showed, that microplastic toxicity was size dependant. Smaller (0.5 μm) particles displayed greater biodistribution and organ accumulation, damaging the spleen, kidney, heart, lung and liver, mainly as a result of excessive accumulation, prompted inflammation and mechanical tissue damage. In contrast, the larger (5 μm) particles caused more damage in the gastrointestinal tract, inducing intestinal barrier dysfunction, reduction of barrier integrity, gut dysbiosis and metabolic disruption (Z. Zhang et al., 2024).

On a cellular level, *in vitro* experiments using human intestinal, lung, immune and other cell lines showed that MNPs can be taken up by cells and may induce production of reactive oxygen species, pro-inflammatory cytokine release, mitochondrial dysfunction, membrane changes, genotoxic stress and altered cellular metabolism. Regardless, severe cytotoxicity was usually observed only at relatively high MNP concentrations with use of pristine laboratory particles that may not fully represent weathered environmental plastics (Yong et al., 2020). Overall MNPs pose potential health risks through various biological pathways. However, the field is developing and direct human health concerns still remain uncertain.

1.3.2. Immunological aspects of small intestine neoplasia development

MNPs have shown to induce or support the presence of inflammation through different pathways. One of these pathways occurs through barrier disruption (Zeng et al., 2024). Its

importance is highlighted by increased intestinal permeability and subsequent exposure of mucosal immune cells to microbial contaminants and inflammatory stimuli (Chen et al., 2024; Zeng et al., 2024). It has been demonstrated, that oral exposure of mice to PS microplastics of 0,2 μm, 1 μm and 5 μm induced oxidative stress and inflammatory cell infiltration in the colon, together with increased pro-inflammatory cytokine expression (Zeng et al., 2024). The same study showed reduced mucus secretion and downregulation of key tight junction proteins, such as ZO-1, occludin and claudin-1, implying structural weakening of the epithelial barrier. It was also demonstrated, that oxidative stress activated NF-κB and the NLRP3-inflammasome, leading to increased IL-1β and IL-18 signalling and infiltration of macrophages and neutrophils into the intestine (Chen et al., 2024; Zeng et al., 2024). This in return contributed to tight-junction disruption and increased permeability. In the intestinal tissue, continuous activation of these pathways can contribute to epithelial injury, immune-cell recruitment and inflammatory signalling (Bruno et al., 2024; Chen et al., 2024). Repeating cycles of epithelial damage and regeneration are relevant for neoplastic development because this increases proliferative pressure on epithelial cells and may favour the survival and expansion of altered clones.

An additional immunological pathway, induced by MNPs, involves platelet activation. A study done by Bruno et al. highlights, that intestinal epithelial damage, caused by MNPs, may activate platelets, which then release lipid mediators, such as thromboxane A2 and prostaglandin E2, as well as cytokines, chemokines, growth factors and extracellular vesicles. This subsequently leads to immune cell, endothelial cell, fibroblast and tumour cell activation, persistence of chronic inflammation and remodelling of tumour microenvironment (Bruno et al., 2024).

Although there is insufficient proof, that MNPs directly cause CRC, experimental and review-based data suggest, that they may contribute to biological processes, that are known to support inflammation-associated tumorigenesis, particularly in high-risk settings, such as inflammatory bowel disease (Bruno et al., 2024). These processes, as mentioned before, might include epithelial barrier disruption, oxidative stress, inflammasome activation, pro-inflammatory cytokine release, immune-cell infiltration, dysbiosis, endotoxin translocation and chronic inflammatory signalling (Bruno et al., 2024; Zeng et al., 2024).

MNPs may act as potential promoters or amplifiers of inflammation-associated intestinal neoplasia, especially where epithelial barrier function and immune homeostasis are already impaired. Future studies are needed to determine, whether chronic, environmentally realistic MNP exposure might directly lead to increased adenoma or carcinoma formation.

1.3.3. Relevance for intestinal tumour development

As MNPs have been identified to enter the human body mainly through ingestion, intestinal mucosa is thus the first major biological barrier that interacts with these particles. Current available evidence does not prove, that MNPs directly cause intestinal cancer in humans, but several studies suggest, that they may contribute to biological conditions, that influence intestinal neoplasia (Bruno et al., 2024; Cetin et al., 2023).

Intestinal barrier damage is considered to be one of the main mechanisms, by which MNPs induce neoplasia (Bruno et al., 2024). Normally, the gut barrier prevents luminal bacteria, endotoxins and harmful particles from entering and damaging the mucosa, while simultaneously maintaining immune tolerance toward commensal microorganisms (Zeng et al., 2024). One study showed, that a combined exposure to different-sized PS particles, especially nanoplastics together with microplastics, produced greater intestinal barrier dysfunction than one-size particle exposure. This effect was caused mainly by ROS-induced epithelial apoptosis, which increased intestinal permeability and enabled greater particle bioavailability (Liang et al., 2021).

In a study, done by Cetin et al., microplastics were found in colon tissues from patients with colorectal adenocarcinoma. Tumorous and non-tumorous colon tissue from the same patient, as well as normal colon tissue from individuals without CRC were compared. Although microplastics were found in all groups, the number was significantly higher in tumorous colon tissue. One possible explanation is, that adenomatous colorectal tissue may retain more particles due to its altered architecture, abnormal vascularization, disrupted extracellular matrix and impaired epithelial barrier function. Nonetheless, the greater quantity of microplastic particles in tumour tissue should be interpreted as an association, but not proof, that microplastics initiate cancer. (Cetin et al., 2023).

A different study, conducted by Bonanomi et al., demonstrated, that normal human colon cells, after being exposed to PS MNPs, subsequently internalised these particles. After

chronic exposure for 28 days with 5 μg/ml of nanoplastics (0.5 μm) or 20 μg/ml of microplastics (2 μm), colon cells exhibited biological properties, resembling cancer-associated metabolic rewiring - increased lactate production through glycolysis (under aerobic conditions), reduced mitochondrial activity, altered ATP production and increased use of glutamine for anabolic processes. This indicates, that, if MNPs induce metabolic patterns in healthy colon cells similar to those in cancer cells, they may contribute to a cellular state, that is more vulnerable to neoplastic transformation, particularly in combination with other carcinogenic factors (Bonanomi et al., 2022).

Gut microbiota may also prove to be an important immunological link between MNP exposure and intestinal neoplasia. Dysbiosis is shown to alter microbial metabolites, increase epithelial stress and promote immune activation, all of which may influence CRC risk (Z. Zhang et al., 2024). While some report microbiota disturbance caused by MNPs, others do not, suggesting, that effects may depend on particle size, dose, exposure duration and experimental design. One study found, that mice, which consumed ~ 80 μg/kg/day of 1 μm PS microplastics, showed no weight loss, detectable particle accumulation in internal organs or major microbiome changes, although mild pro-inflammatory transcriptional changes were detected in the colon (Rawle et al., 2022).

To conclude, based on available data, MNPs should initially be considered as potential tumour-promoting environmental stressors, rather than direct carcinogens. Their physiological impact may be especially relevant in individuals with chronic intestinal inflammation, impaired barrier function or inflammatory bowel disease.

2. Research aim and objectives

Given that CRC is the third most commonly diagnosed cancer-type and the second leading cause of cancer death in the United States of America alone (Siegel et al., 2026), it is important to investigate the possible effects, that plastic particles – one of the most prevalent modern environmental pollutants (Barnes et al., 2009) – might have on its development. Considering, that MNPs enter the human organism mainly via ingestion and inhalation and thus commonly transverse the gastrointestinal tract (Dick Vethaak & Legler, 2021), there is a high possibility that a number of toxicological events take place. Some studies described an accumulation of microplastic in healthy and cancerous human colon tissue (Cetin et al., 2023), MNP internalisation in healthy human colon cells with ensuing oxidative stress and metabolic rewiring (Bonanomi et al., 2022), stronger intestinal barrier dysfunction after a exposure to a combination of PS MNPs displayed in mice (Liang et al., 2021), activation of inflammatory signalling, increased IL-1β and IL-18 liberation, reduction in tight-junction proteins and increased intestinal permeability (Chen et al., 2024). Small intestine neoplasia, on the other hand, is not as prevalent and frequent as CRC, but it displays similar tumorigenic pathways (Aparicio et al., 2022b). One of these pathways is the APC gene mutation, which causes FAP syndrome in humans and the development of multiple colon adenomas. Simultaneously, this mutation yields multiple adenomatous polyps in the small intestine of mice (Moser et al., 1995). Due to this molecular similarity, the $APC^{Min/+}$ mouse model was developed in order to mimic the human FAP syndrome (Li et al., 2022). This makes it the perfect experimental *in vivo* subject for examination of MNPs impact on intestinal neoplasia.

The aim of this thesis was to investigate long-term effects of MNPs-ingestion on intestinal polyp formation and progression, based on an $APC^{Min/+}$ mouse model. The overall survival, physical variations, histopathological assessment of polyps and immunological effects were compared, as well as MNP accumulation in small intestine tissue examined.

3. Material and Methods

A list of chemicals, reagents and devices, which were used in the following experiments are listed in Appendix section 8.1.

3.1. $APC^{Min/+}$ mouse model

In order to investigate the potential effects of MNP exposure on intestinal neoplastic development, $APC^{Min/+}$ mice were selected (for details on the model please see chapter 1.1.5). The initial strain of heterozygote $APC^{Min/+}$ male mice was ordered from The Jackson Laboratory (Bar Harbor, ME, USA; stock no. 002020) and delivered to the Core Facility Laboratory Animal Breeding and Husbandry of the Medical University of Vienna for consecutive breeding. $APC^{Min/+}$ males were paired with C57BL/6J wild-type females for mating in a specific pathogen-free facility. Several days after birth mouse pups were toe-clipped for subsequent identification and genotyping. Given that that there´s an equal probability for mutant as well as wild-type offspring, genotyping was conducted.

3.1.1. Genotyping

3.1.1.1. DNA extraction

Postnatal mouse pup toe clips were done by the facilities animal caretakers and provided in labelled 1.5 ml Eppendorf test tubes at temperature -20°C. Subsequently DNA-extraction was initiated by adding 500 µl Lysis buffer (Appendix, section 8.1, Supplementary Table 6) along with 15 µl of 10 mg/ml Proteinase K to each test tube. The samples were then vortexed, sedimented and incubated at 54°C with shaking at 850 rotations per minute (rpm) for a minimum of 2-2.5 h. After complete tissue digestion 200 µl 5 M NaCl were added to each test tube, vortexed and centrifuged at 15 000 rpm for 10-15 min at room temperature conditions. This step achieved pelleting of cellular debris and precipitated proteins, while soluble genomic DNA remained in the supernatant. Around 600 µl supernatant were then carefully transferred to new, accordingly labelled test tubes and an equal volume (600 µl) of isopropanol was added. The samples were then centrifuged at 15000 rpm for 32 min at room temperature conditions. Isopropanol significantly reduces DNA solubility and causes it to precipitate while a clear pellet is formed through centrifugation. After discarding the supernatant, each pellet was washed with 300 µl pre-cooled 70% ethanol to remove any

soluble contaminants. Samples were then centrifuged again at 15 000 rpm for 5 min at room temperature. Afterwards the supernatants were discarded and test tubes containing the DNA-pellet left to air dry at room temperature. Subsequently the pellets were resuspended in prewarmed nuclease-free water and incubated at 34°C for 2h. These samples were then stored at 4°C short-term or at -20°C long-term.

3.1.1.2. Polymerase chain reaction (PCR)

After completed DNA extraction a PCR-mix (Appendix, section 8.1, Supplementary Table 1) of Diethylpyrocarbonate(DEPC)-treated water, 5x PCR reaction buffer containing Mg^{2+}, 10 µM APC-HindIII forward primer, 10 µM APC-HindIII reverse primer, 10 mM dNTP mix and HS Taq DNA Polymerase M101 (5000 U/ml) was prepared for all samples and two controls, and aliquoted at 24 µl per sample to labelled PCR test tubes. 1 µl of each DNA extraction solution was added to the respectively labelled PCR test tubes. Additionally, a positive and negative control (Ctr) was prepared in advance from a known $APC^{Min/+}$-positive and a wildtype C57BL/6J mouse and 1 µl sample was also added to the PCR-solution mix in the correspondingly labelled test tubes. These test tubes were then placed into C1000 Touch Thermal Cycler and set for a PCR thermocycling program as shown in Table 1.

Table 1: PCR thermocycling program

Run	**1**	**2**			**3**	**4**
Cycle count	1	40			1	1
Temperature	95°C	95°C	50°C	68°C	68°C	4°C
Time	5 min	30 s	30 s	40 s	3 min	∞

3.1.1.3. HindIII digestion

Following PCR program a mix (Appendix, section 8.1, Supplementary Table 2) of DEPC-treated water, 10x NEBuffer™ r2.1 and HindIII (20000 U/ml) solution was created and aliquoted at 8 µl to labelled PCR test tubes for HindIII (Type II restriction endonuclease isolated from Haemophilus influenzae) digestion. Information about used materials and reagents can be found in Appendix section 8.1. 12 µl of each finished PCR thermocycling

solution was added to respectively labelled HindIII test tubes, placed into C1000 Touch Thermal Cycler and set for a thermocycling program at 37°C for 3h.

3.1.1.4. Electrophoresis

For analysis of the DNA product 3 g agarose were mixed with 100 ml of 1x Tris-acetate-EDTA (TAE) buffer (appendix section 8.1, Supplementary Table 7) in a glass beaker and microwaved for approximately 2 min. Avoiding bubble formation the beaker was gently swirled under running tap water in order to cool down. Once the agarose gel cooled and the beaker was at a hand-warm handling temperature 10 µl of prediluted Midori Green Advanced stain (0.01 µl/ml) were mixed in the gel, solution was poured into a casting tray and allowed to solidify. Once the HindIII digestion was finished 4 µl of 6x DNA loading dye were added to each of the test tubes and mixed thoroughly through resuspension. 7 µl Quick-Load® purple 100 bp DNA ladder and 20 µl each of the HindIII digestion solution mix with loading dye were pipetted on the agarose gel and run at 130 V for around 1.5 h. The images were afterwards taken with ChemiDoc MP Imaging System. An example of a post-electrophoresis agarose gel is shown in Figure 2. Due to an insertion of a HindIII restriction site using PCR primers in wild-type mice, corresponding bands are shorter, whereas in the case of a mutation, no restriction site is formed thus the PCR product is not cleaved and appears longer (Figure 2). As $APC^{Min/+}$-positive mice are heterozygous and also contain a wildtype allele, a double band is visible in these mice.

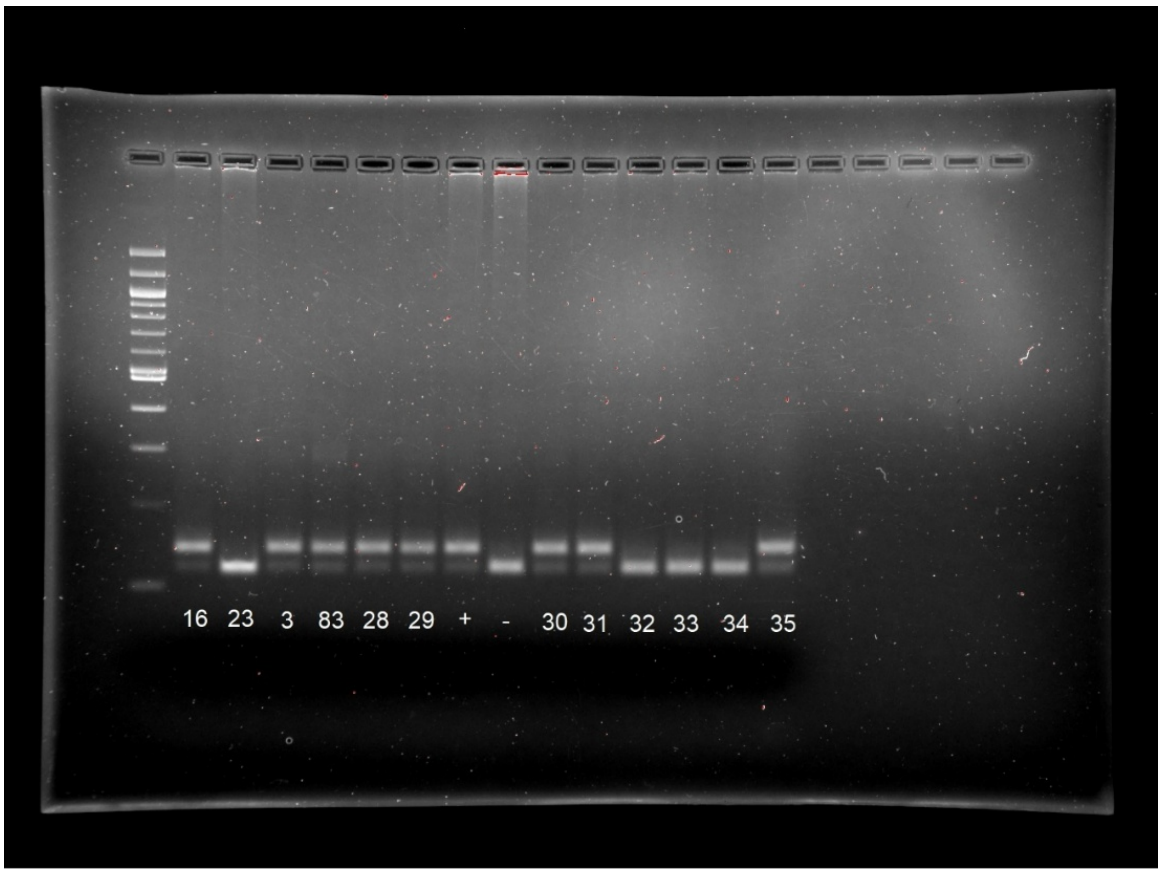

Figure 2: Post-electrophoresis 3% agarose gel with genotyping results. Positive ($APC^{Min/+}$ mouse) and negative (C57BL/6J mouse) Ctr marked as + and – respectively. Lines labelled as mouse toe clip numbers. Positive bands are visible at 150 bp and negative at 120 bp.

3.1.2. Husbandry procedures

After reaching around three weeks of age, mice pups were separated from their mother, randomized according to their genetic status into experimental groups and transferred from breeding specific pathogen-free area to experimental rooms which had conventional barrier housing with filtertop cages. Taking into account their social nature, mice were held in groups of at least two individuals in hanging cages at room temperature with 12 h light/dark cycle. Food and water were provided ad libitum. The cages were cleaned by staff once a week. All experiments were conducted according to Austrian animal welfare legislation (license 2022- 0.257.045), and experimental setups were approved by the local animal ethics committee.

3.2. Plastic particles

3.2.1. PS MNP particles

Fluorescently labelled round PS particles were used for both experiments. Three different particle sizes at approximately 10 µm, 1 µm and 0.3 µm were purchased prior to treatment initiation. For more detailed information see Table 2.

Table 2: Information about the MNP particles used for the experiments.

Product Name	Product ID	Size	Colour	Concentration	Manufacturer
PS 10 µm particles	PS-FB-Fi365	10.39 µm ± 0.13 µm	Blue (brightfield)	5 % (w/v)	Microparticles GmbH (Germany)
PS 1 µm particles	PS-FluoRot-Fi296	1.16 µm ± 0.03 µm	Fluo-red *(Ex/Em = 530/607 nm)*	2.5 % (w/v)	Microparticles GmbH (Germany)
PS 0.3 µm particles	PS-FluoGrün-Fi255-1	0.293 µm ± 0.008 µm	Fluo-green *(Ex/Em = 502/518 nm)*	2.5 % (w/v)	Microparticles GmbH (Germany)

3.2.2. Preparation of MNP mouse food

Regular corn-based mouse food (LASQCdiet® Rod16-A, Altromin Spezialfutter GmbH & Co. KG, Lage, Germany) pellets were put into a stationary blender and crushed to a powdery appearance. Mouse food powder was then transferred into a dough mixer bowl. The powder was pre-wet and a PS-MNP mix (10 µm, 1 µm and 0.3 µm) solution was gradually added to the mass (0.1 mg of each type MNP per 1 g mouse food) and mixed until homogenisation (Appendix, section 8.2, Supplementary Figure 1, A). Afterwards, using a meat grinder with a sausage adaptor long strands of mouse food were formed and cut into pellets (Appendix section 8.2, Supplementary Figure 1, B). The trays with mouse food were then placed into an incubator and dried for 72 h at 56°C. Dried MNP mouse food pellets were then packed into double layers of plastic bags and, as a final step, transported to Mediscan GmbH (Seibersdorf) for sterilization by gamma irradiation (25 kGy).

3.3. Experimental design

3.3.1. 100-day experiment

The purpose of this experiment was to observe and analyse possible physiological and histological effects that MNPs have on intestinal neoplasia for a fixed period of time. A total of 25 $APC^{Min/+}$ mice (15 females and 10 males) were randomly divided into two treatment groups. Ctr groups consisting of 7 females and 4 males respectively and treatment (MNP) groups consisting of 8 females and 6 males as shown in Table 3.

Table 3: Overview of treatment groups for the 100-day experiment.

Experimental group	Ctr ♀	Ctr ♂	MNP ♀	MNP ♂
Number of mice	7	4	8	6

Mice were between 3 to 6 weeks of age at the start of the experiment. Ctr mice received regular corn-based mouse food and treatment mice provided with the MNP supplemented food of 0,3 mg MNP mix/g in mouse feed; average food consumption ~ 3 g daily, resulting a daily MNP dose of ~ 0.9 mg. For the duration of the experiment, body weight measurements and clinical assessments were conducted. At the experimental endpoint on day 100, all surviving subjects were euthanized in accordance to animal welfare protocols and organs were collected for subsequent analysis.

3.3.2. Survival experiment

With the aim to assess long-term effects of MNPs on intestinal neoplasia an additional survival study was conducted. $APC^{Min/+}$ mice are known to live an average of 120 days (Moser et al., 1995). The objective was to analyse, what effect MNP has on overall life expectancy, immune reaction to and progression of intestinal neoplasia in $APC^{Min/+}$ mice. A total of 35 $APC^{Min/+}$ mice (19 females and 16 males) were randomly divided into two treatment groups as shown in Table 4.

Table 4: Overview of treatment groups for the Survival experiment.

Experimental group	Ctr ♀	Ctr ♂	MNP ♀	MNP ♂
Number of mice	9	8	10	8

Mice were between 6 to 13 weeks of age at the start of the experiment. According to the procedures for the previous experiment Ctr mice received regular corn-based mouse food and treatment mice were provided with MNP-supplemented food (0.3 mg MNP mix/g mouse feed; average food consumption ~ 3 g daily). Similarly, for the duration of the experiment, body weight measurements and clinical assessments were conducted. Due to the nature of this experiment, there was no fixed endpoint and the experimental run was terminated individually upon having reached pre-defined termination criteria. After notable overall health deterioration, as will be described in the following section 3.4.2, or a loss of 20% of body weight relative to the previous weeks mice were euthanized in accordance to animal welfare protocols, marking their individual endpoint, and organs were collected for subsequent analysis.

3.4. Subject monitoring

3.4.1. Longitudinal body weight measurement

Over the course of both experiments, mouse body weight was documented on average every 2-3 days. If a mouse had shown visible health deterioration together with body weight decline of more than 10% then measurements would be made daily until sampling. To reduce the risk of cross-contamination with MNPs, Ctr groups were assessed before MNP-treated groups. For weight measurements, mice were gently restrained by grasping skin at the nape of the neck, which enabled identification of the individual mouse based on clipped toes and an overall health assessment. They were afterwards gently transferred to an empty tarred cage on the scale by lifting them on the base of the tail as shown in Figure 3.

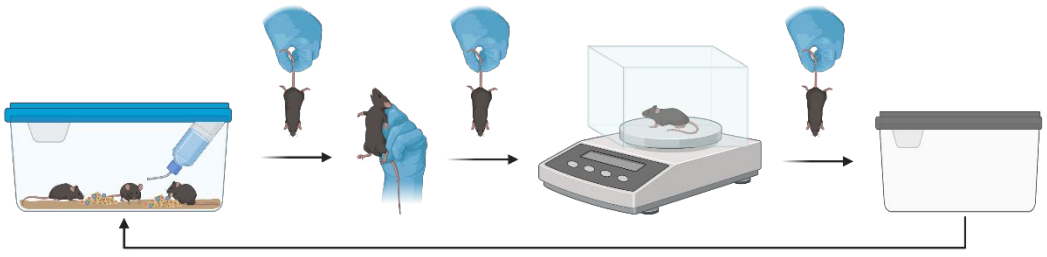

Figure 3: Schematic illustration of mouse health check-up and body weight measurement process. Created with BioRender.com.

3.4.2. Clinical assessment

The $APC^{Min/+}$ mouse model is known to develop anaemia and intestinal bleeding along disease progression. A special clinical scoring system (Table 5) was created for the purpose of assessing the health status of experimental mice and determining humane endpoints. Clinical scorings were performed alongside mouse body weighing. A score of 0-2 indicated a stable health condition, whereas a score of 3-6 required daily monitoring. All mice with a daily score of more than 7, loss of more than 20% of body weight or loss of the righting reflex were immediately euthanised.

*Table 5: Clinical scoring system for $APC^{Min/+}$ mice. Physical changes marked with "**" required immediate euthanasia.*

Parameter	Physical changes	Score
Body weight (relative to average weight in the 2 weeks before)	Weight gain or no changes	0
	<10% loss	1
	10-15% loss	2
	15-20% loss	3
	>20% loss**	4
Physical condition	No changes	0
	Pale mucosa, slight hunching	1
	Pale mucosa, blood in faeces, diarrhoea, pale paws (anaemia)	2
	Changes from above + bloated abdomen	3
	Shaggy fur, lack of grooming, abnormal posture	4
Behaviour	No changes	0
	Reduced activity, reaction to mild external stimuli	1
	Reduced activity, reaction to moderate external stimuli (slow movement)	2
	Loss of righting reflex (within 5 seconds) **	4

3.5. Sample collection

3.5.1. Euthanasia and necropsy

After reaching the experimental endpoint, mice were euthanised with an overdose injection of Ketamin (150 mg/kg) and Xylazin (15 mg/kg). Promptly after reflexes are lost and breathing had stopped, blood collection was performed via cardiac puncture and subsequent dissection. Ctr mice were processed prior to MNP-treated mice. To avoid cross-contamination two separate sets of dissection instruments were used for treatment groups. Organs were harvested, macroscopically assessed and weighed. Although most organs were collected, detailed histopathological analysis focused only on small intestine and spleen. For the small intestine and colon, the inner lumen was additionally gently flushed firstly with PBS using a syringe with a pipette tip in order to remove faecal material and afterwards once again with a 4.5% formaldehyde (PFA) solution. It was then positioned into a histological cassette on a piece of filter paper in a "Swiss roll" form with the distal end being in the centre.

Only one male MNP mouse from the 100-day experiment was sampled 15 days before the experimental endpoint due to a subcutaneous tumour on its hind leg. Similarly, one mouse from the survival experiment was excluded from necropsy as it was found dead in the cage (unforeseeable exitus) and organs had already started to decompose.

3.5.2. Organ processing

Following dissection, organs were put into accordingly labelled histological cassettes and submerged in 4.5% PFA solution for 24-48 h. Samples from Ctr mice and MNP-treated mice were divided into two separate containers with the aim of preventing contamination with MNPs (this was then effective for all further processing steps). After 24-48h the samples were either transferred to 0.2% PFA for longer storage in the fridge or further processed in accordance to the protocol by Gonçalves et al., 2018. Cassettes were put in fresh purified water for 15 min (this step was repeated 3 more times). Then they were transferred to 70% aqueous isopropanol for 30 min. Afterwards they were placed into 95% aqueous isopropanol solution for 15 min (this step was repeated two more times). Next the samples were submerged in 100% isopropanol with vacuum for 1 h (this step was repeated two more times). Finally, samples were placed into warm liquid paraffin, added vacuum for about 10 min or until the air bubbles stopped emerging and left in the incubator at 56°C for 24 h.

3.6. Histological tissue processing

After completed paraffin infiltration, organ samples were neatly positioned into pre-warmed metal casting molds and embedded in paraffin using Tissue-Tek® TEC™ 6 Embedding Module as shown in Supplementary Figure 2 in appendix section 8.3. Completed and cooled tissue blocks were then cut at 3 μm using Microm HM 340E microtome and mounted on glass slides as shown in Supplementary Figure 3 in appendix section 8.3. Priority was given to Ctr treatment samples, whereas used devices were thoroughly cleaned after processing of MNP-treatment samples. Freshly mounted glass slides were left to air dry for 24 h. A schematic representation of main organ processing steps is shown in Figure 4.

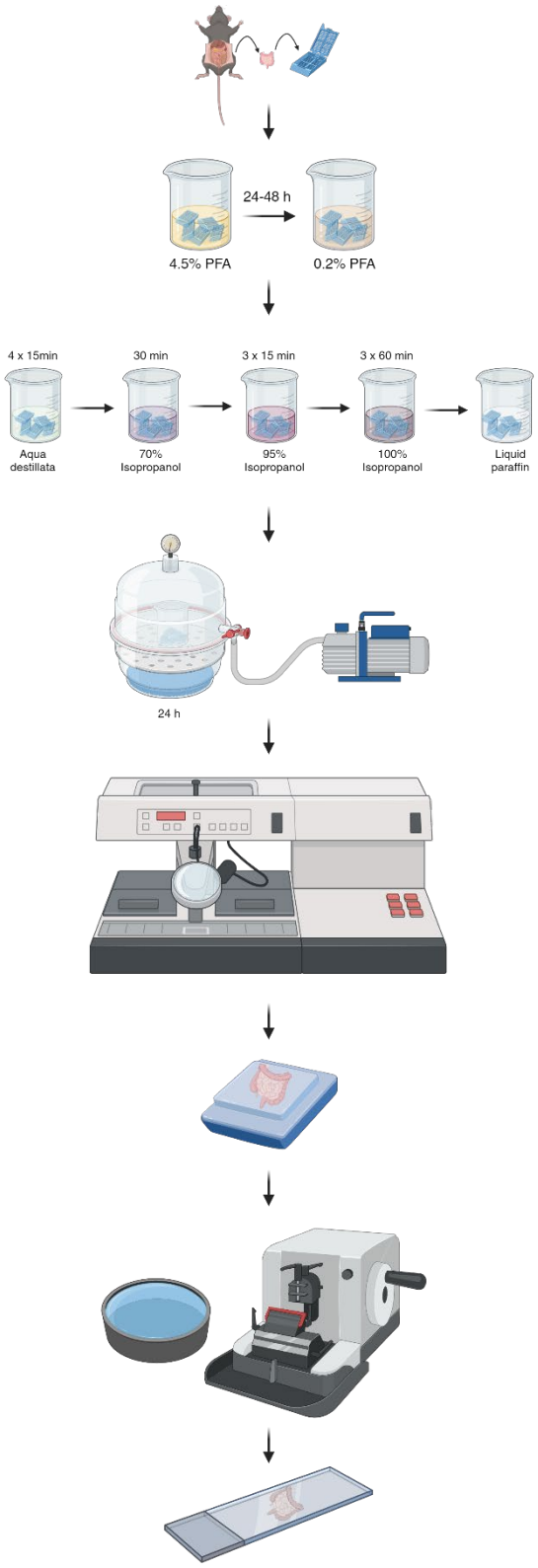

Figure 4: A schematic representation of the tissue processing workflow in preparation for subsequent histological staining. Created with BioRender.com.

3.7. Tissue staining

3.7.1. Haematoxylin and Eosin (H&E) staining

H&E-stained sections were used for morphological assessment and histopathological grading of polyps in small intestine, based on their structural and cellular features. First part of H&E staining was comprised of deparaffinisation steps. Mounted slides were placed in an incubator at 56°C for 1.5 h. After the paraffin had sufficiently melted, the slides were then taken to the staining line (Table 6) and submerged in three consecutive xylene solutions for 15 min each. Slides were then rehydrated by brief repeated immersion through decreasing ethanol concentrations followed by a 5 min submersion in purified water. Sequentially the slides were placed in Mayer's hemalum solution for 5 min and afterwards dipped in fresh tap water in order to remove excess staining solution. After a following 15 min nuclear blueing in Scott's solution, sections were counterstained for 2 min with acidified eosin, rinsed twice in fresh purified water, dehydrated through an increasing ethanol series, submerged in n-butyl acetate and mounted with Eukitt® mounting medium. Slides were then let to air dry in the fume hood.

Table 6: Schematic structure of H&E staining line. Numbers below represent time in minutes.

Xylene	Xylene	Xylene	100% EtOH	100% EtOH	96% EtOH	70% EtOH	50% EtOH	Aqua destillata	Haematoxylin	2x tap water	SCOTT solution	Eosin	2x Aqua destillata	96% EtOH	100% EtOH	n-butyl acetate
15	15	15	/	/	/	/	/	5	5	/	15	2	/	/	/	/

3.7.2. Immunohistochemical staining

To further evaluate immune-related changes within the small intestinal tissue, immunohistochemical staining was performed for F4/80, Arg1, iNOS, and neutrophil elastase. These markers were selected to assess macrophage and neutrophil infiltration in intestinal tissue, especially adenomatous polyps. Specifically, F4/80 served as a macrophage-associated marker, Arg1 and iNOS were used as indicators for macrophage-specific polarized subpopulations (anti- and pro-inflammatiory phenotype) and neutrophil elastase was used to detect neutrophil-associated inflammatory responses.

With the help of a laboratory technician – Ms. Michaela Schlederer - DAB-based detection protocol was used for immunohistochemical staining with F4/80, Arg1, iNOS, and neutrophil elastase markers (antibodies listed in Supplementary Table 9 in appendix section 8.4). Mounted sections were deparaffinized in xylene and rehydrated through a descending ethanol series. Afterwards, the tissue area was encircled with a hydrophobic barrier pen and washed in Tris-buffered saline with Tween® 20 (TBS-T). Heat-induced antigen retrieval was performed in either citrate or TRIS-EDTA buffer by being microwaved at 600 W for 20 min, followed by cooling at room temperature. From this step onward, sections were kept moist throughout the staining procedure.

Slides were then incubated with 3% H_2O_2 for 10 min at room temperature in order to inhibit endogenous peroxidase. After repeated washing in TBS-T, sections were incubated with a blocking solution for 1 h at room temperature, in order to reduce non-specific binding. Primary antibodies against previously mentioned markers were applied at antibody-specific dilutions and incubated overnight at 4°C in a humidity chamber. Negative Ctr sections were parallelly incubated with the corresponding control rabbit IgG-Antibody at the same dilution as the respective primary antibody.

The following day, sections were washed in TBS-T and incubated with the appropriate biotinylated secondary antibody for 1 h at room temperature. Afterwards, an ABC reagent was applied for 30 min, followed by chromogenic detection with DAB until visible colour development occurred. Sections were rinsed in distilled water, counterstained with haematoxylin, dehydrated through an increasing ethanol series, cleared in xylene and eventually mounted with Eukitt® mounting medium - similar as described for H&E staining procedure before.

3.7.3. Fluorescence staining

Given that the PS-MNP particles used in this study were fluorescently labelled, fluorescence staining of nuclei was performed on small intestinal sections to assist microscopic detection and localization. This enabled descriptive assessment of particle distribution and potential accumulation within the intestinal tissue. A special sample processing protocol had to be followed in order to preserve the PS plastic particles, which would be otherwise dissolved when using xylene for clearing. Deparaffinisation and rehydration steps of mounted paraffin samples were performed in accordance to a pre-defined protocol (Gonçalves et al.,

2018). Slides were heated up on a 65°C hot plate and repeatedly immersed in 100% isopropanol solution in between heating in order to effectively and completely remove paraffin residue. Successive rehydration steps consisted of 2 x 1 min immersion in 95% isopropanol, 30 s immersion in 70% isopropanol and final 6 min submersion in purified water. Afterwards the tissue on the slide was encircled with a hydrophobic pen, covered with a few drops of aqueous 1:1000 dilution of 1 mg/ml Hoechst fluorescent nucleic acid dye and left for 10 min in the dark. Samples were subsequently washed twice with purified water and mounted with permanents aqueous mounting medium to be stored at 4°C until further analysis.

3.8. Microscopic analysis

3.8.1. Staining evaluation

H&E and immunohistochemically stained samples were scanned with an Olympus SLIDEVIEW™ VS200 (Evident, Tokyo, Japan) slide scanner. With the use of QuPath v.0.5.0: open-source software for digital pathology image analysis (Bankhead et al., 2017) the total area of longitudinally sectioned, H&E-stained small intestine tissue was analysed and annotated.

$APC^{Min/+}$ mice are reported to develop on average around 30 adenomas in the small intestine and only few in the colon by the time they reach 4 month of age (Boivin et al., 2003). In accordance with the study objective and the selected experimental mutant mouse model, which is predisposed to spontaneous intestinal adenoma formation, focus was placed on analysis of polyps in the small intestine. Figure 5 presents a microscopic overview of an H&E-stained longitudinal section of a Swiss-rolled small intestine belonging to a MNP-treated mouse. A total of 34 polyps, marked with arrows, can be seen in the image. Said polyps seem to be more concentrated to the centre of the “Swiss-roll”, which is closer to the distal end of the small intestine.

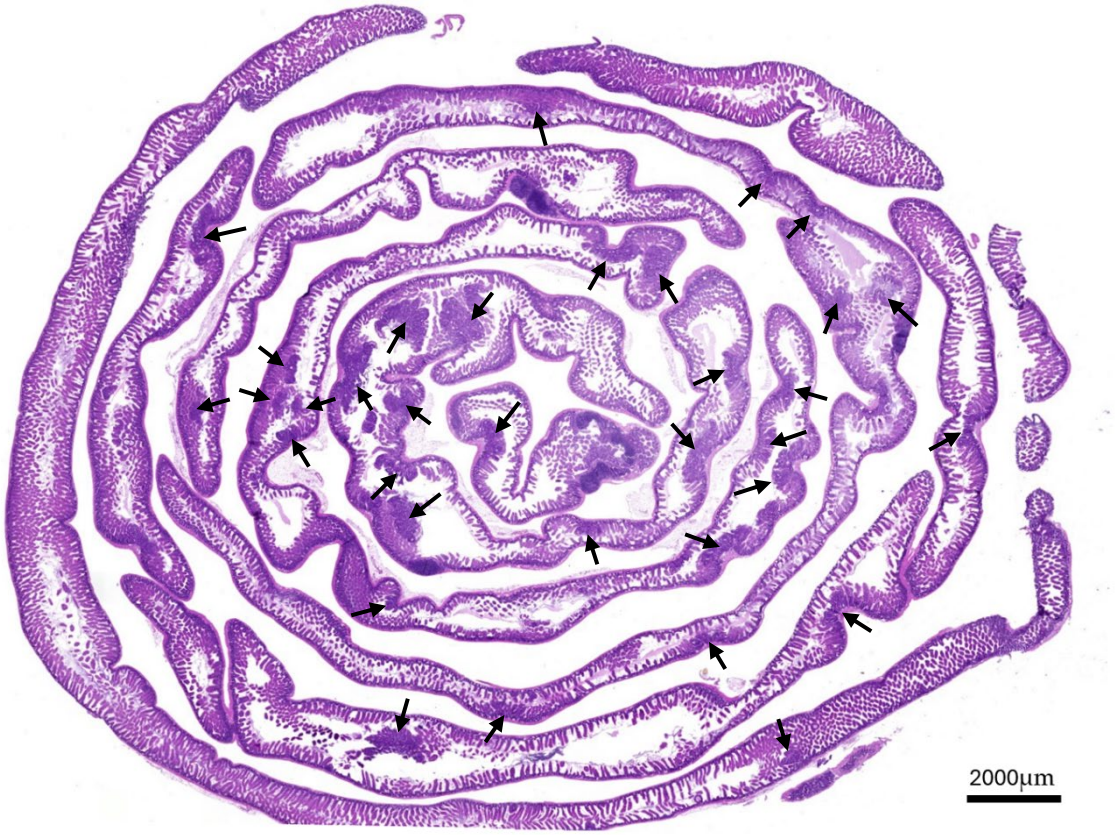

Figure 5: Overview of a H&E-stained Swiss-rolled small intestine longitudinal section of an APCMin/+ mouse. Arrows point at intestinal adenomas which are specific to this mouse model.

Total small intestine area was determined by QuPath based software algorithm, while polyps were manually identified and annotated. Per individuum the size and number of polyps was determined as well as the tumor load (% of total area of all polyps normalized to overall small intestine tissue area). With the help of a pathology specialist, intestinal polyps were scored to assess their severity (for details see section 3.8.2).

Immunohistochemically stained samples were visually inspected using the CaseViewer software v2.4 (3DHISTECH Ltd., Budapest, Hungary), as quantitative assessment was not feasible due to staining artefacts from paraffin residues. Staining patterns were only descriptively compared between the two treatment groups.

Fluorescently stained small intestine tissue sections were qualitatively examined for presence of MNPs via Axio Imager M2 (Carl Zeiss AG, Germany) microscope. In process of manual inspection, representative microscopic images were taken of MNP-positive tissue sections for descriptive evaluation.

3.8.2. Polyp scoring

Small intestinal polyps from $APC^{Min/+}$ mice were analysed in H&E-stained sections by a trained pathologist – Univ.-Prof. Dr. Lukas Kenner - and severity score was assessed for each polyp based on cell architecture, cellular density, goblet cell loss, nuclear atypia, loss of epithelial polarity, and evidence of invasion. Low-grade adenomas displayed a recognizable tubular architecture with moderate dysplastic changes. High-grade adenomas exhibited complex glandular architecture, including back-to-back or cribriform glandular formations, marked loss of polarity, goblet cell reduction and distinct nuclear abnormality. Invasive carcinoma was diagnosed only when neoplastic infiltration evidently extended beyond the muscularis mucosae into deeper intestinal wall layers.

A H&E-stained intestinal tissue comparison (Figure 6) between an adenomatous polyp and healthy tissue demonstrates evident morphological differences. Adenomatous regions (B, D) exhibited architectural distortion, irregular glandular organization and epithelial proliferation. In contrast, healthy intestinal tissue (A, C) showed typical villus and crypt structure and regular epithelial arrangement.

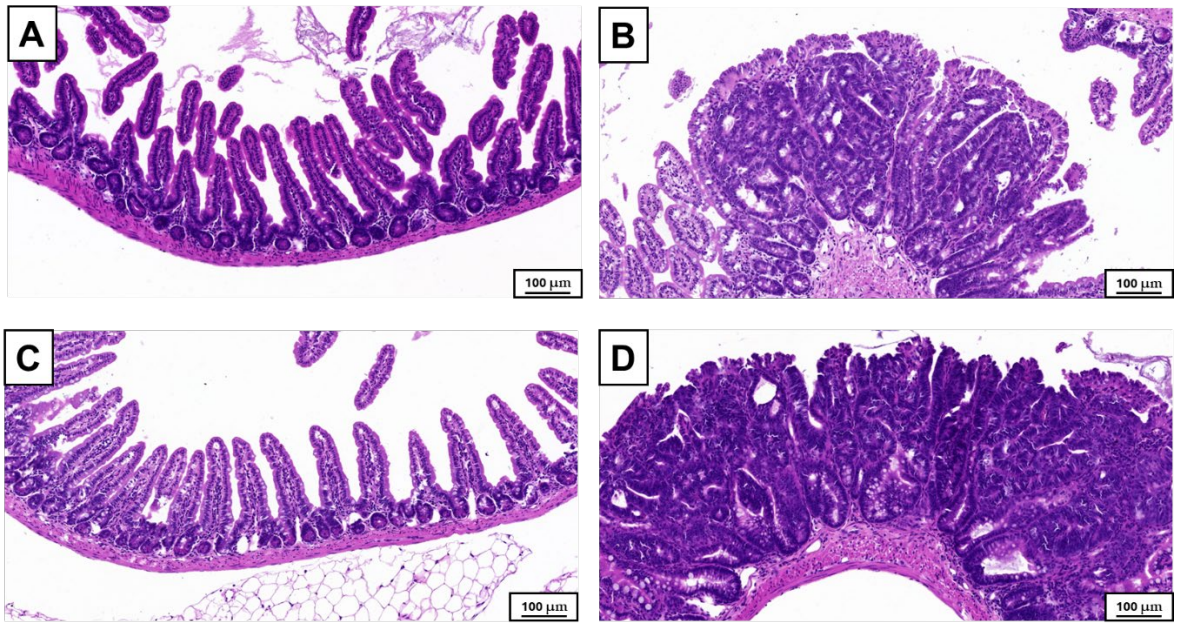

Figure 6: A side-by-side visual comparison of morphological differences between healthy tissue (A, C) and neoplastic intestinal tissue with an adenomatous polyp (B, D).

3.9. Statistical analysis

Quantitative data acquired with previously described methods was further analysed using GraphPad Prism version 9.3.0 for Windows (GraphPad Software, San Diego, California USA). Longitudinal body weight data were analysed using a Mixed-effects Model (restricted maximum likelihood (REML)) with Šídák's multiple comparisons test. For terminal endpoint parameters, such as end weight comparison, tumour load, average polyp area, polyp count and spleen weight, a Shapiro-Wilk test for data distribution was conducted. If data were normally distributed across all groups, comparisons were performed using an unpaired t-test with Welch's correction, whereas, if at least one group displayed non-normality, data were analysed using the non-parametric Mann–Whitney test. Due to a small sample size, both parametric and non-parametric tests are valid for statistical analysis based on normal distribution of the data. Intestinal polyp scoring was analysed using a Mixed-effects Model (REML). Results were considered statistically significant at $p < 0.05$.

4. Results

4.1. 100-day Experiment

4.1.1. Longitudinal body weight trajectory

With the aim to assess preliminary long-term effects of MNP on intestinal neoplasia a 100-day defined time period experimental run was conducted. Considering, that this mouse model was known to survive an average of 120 days(Moser et al., 1995), with increasing health complications as time progressed, it was decided to set the experimental endpoint at 100 days of age, when mice are still in a good physical shape, but polyps have already evolved. During this period a total of 25 $APC^{Min/+}$ mice (15 females and 10 males) were split into experimental groups depending on their sex and treatment (details for grouping see Material & Mehtods section 3.3.1, Table 3). Ctr groups received normal corn-based mouse food, while MNP-treated groups received corn-based mouse feed supplemented with 0.3 mg MNP-mix (3 different sizes at equal weight) per 1 g feed. Depending on their clinical assessment score mice were weighed and health status assessed 3 to 7 times per week. To determine whether body weight changes differed between treatment groups, weight measurements were documented systematically and analysed with GraphPad Prism v9.3.0. after the experimental endpoint.

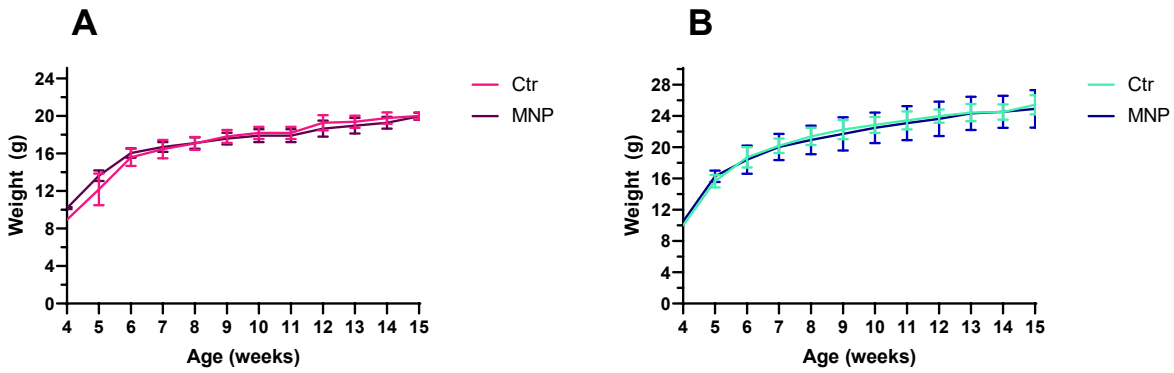

Figure 7: 100-day experiment longitudinal body weight trajectory comparison for both sexes between treatment groups. Graphical depiction of female (A) and male (B) Ctr and MNP group body weight development with increasing mouse age.

Both treatment groups displayed comparable body weight trajectory tendencies as demonstrated in Figure 7. Collected data were statistically analysed using Mixed-effects Model (REML) with Šídák's multiple comparisons test. No statistically significant differences were observed neither for females ($p = 0.8683$), nor for males ($p = 0.8434$).

Additionally, a statistical experimental endpoint body weight comparison was made to identify possible differences between said groups. One male MNP mouse was sampled 15 days before the experimental endpoint due to a subcutaneous tumour and was excluded from the analysis.

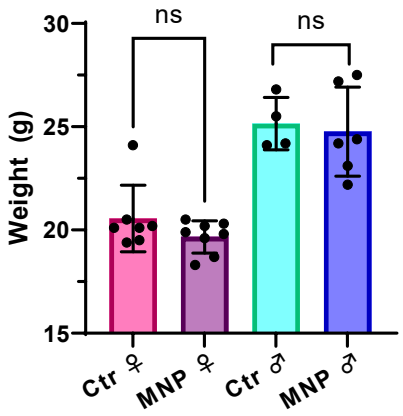

Figure 8: 100-day experimental endpoint body weight comparison between all four experimental groups. Sex specific analysis was done using a non-parametric Mann-Whitney test and indicated no significant difference regarding MNP treatment.

Obtained results did not exhibit statistically significant variances between Ctr and MNP-treated groups in either sex (females $p = 0.4457$; males $p = 0.9667$) as shown in Figure 8.

Statistical comparison of body weight differences was conducted separately for both sexes as male mice have a natural tendency to grow larger and heavier than females (mean end weight: females ~ 20 g vs. males ~ 25 g). Graphical longitudinal body weight development curves were nearly identical between Ctr and MNP-treated mice in both sexes, which indicates no notable effect of MNP on weight gain over time. MNP-food was well tolerated, as indicated by equal weight gain, and did not result in any obvious health associated features upon long-term exposure. Furthermore, the comparative statistical endpoint body weight analysis demonstrated no significant differences between treatment groups for both sexes.

4.1.2. Spleen weight assessment

Given that the immune system plays a major role in controlling the expansion of cancerous cells and to monitor inflammatory processes, as an additional physiological endpoint parameter, it was decided to look into possible differences in spleen weight between treatment groups. As it is one of the main lymphoid organs involved in immune regulation and inflammatory responses, potential weight changes may suggest tumour-associated systemic inflammation, immune activation or changes in hematopoietic activity.

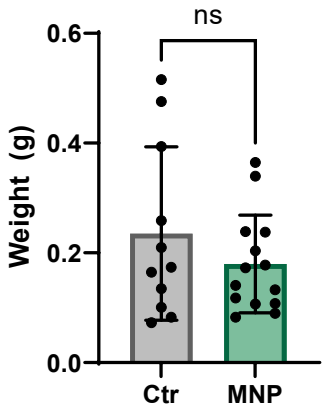

Figure 9: 100-day experiment spleen weight differences between treatment groups.

Although mean spleen weight was lower in the MNP treated group (0.1798 g), than in the Ctr group (0.2351 g), statistical analysis exhibited no statistical significance ($p = 0.3154$) as shown in Figure 9. It has been directly shown that $APC^{Min/+}$ mice develop chronic anaemia, which is usually associated with splenomegaly as a compensatory mechanism, which also results in increased spleen weight compared to wildtype mice (Ren et al., 2019; Shepherd et al., 2020). In addition, a study conducted by Shepherd et al. showed, that $APC^{Min/+}$ mice, who were around 5 months of age, had on average significantly heavier spleens (~ 0.5 g) than their 6-month-old C57Bl/6J wildtype counterparts (~ 0.08-0.12 g) (Shepherd et al., 2020). Overall, both anaemia and inflammation – later resulting probably either from damaged intestinal barrier due to polyp growth or MNP application – might directly influence the increase in spleen weight.

4.1.3. Small intestine polyp burden

The $APC^{Min/+}$ mouse model was intentionally chosen for this study, due to its genetic mutation, which induces spontaneous formation of intestinal adenomas, preferentially in the small intestine. This makes it a suitable *in vivo* system for assessment of neoplasia-

associated morphological and immunological changes in small intestine and for evaluation of potential effects MNP-exposure has on intestinal cancer progression.

H&E-stained samples were scanned and then analysed with QuPath v.0.5.0 software. For each experimental mouse the total area of a small intestine longitudinal section was annotated automatically, whereas intestinal polyps had to be manually assessed and separately annotated. Tumour load, average polyp area and polyp count counts per individual were assessed. Polyp count represents the number of intestinal polyps identified per analysed longitudinal small intestine section. Average polyp area was calculated by adding all identified intestinal polyps for every mouse and dividing them through individual polyp count. These findings, however, might not be fully accurate due to the fact that polyps bordered one another, which made it difficult to properly discriminate from HE sections the exact boarders of individual polyps, which grew in close proximity.

Tumour load was assessed by computing the percentage share of cumulative intestinal polyp area in relation to total area of the small intestine section. As no sex differences were observed regarding these parameters (data not shown), obtained data were only grouped according to exposure (Ctr and MNP). The results showed no statistical significance in accordance to treatment for either polyp count ($p = 0.5082$), tumour load ($p = 0.7521$) or average polyp area ($p = 0.0885$). The latter, however, displayed a slight trend towards lower average polyp area in MNP-treated mice (Figure 10).

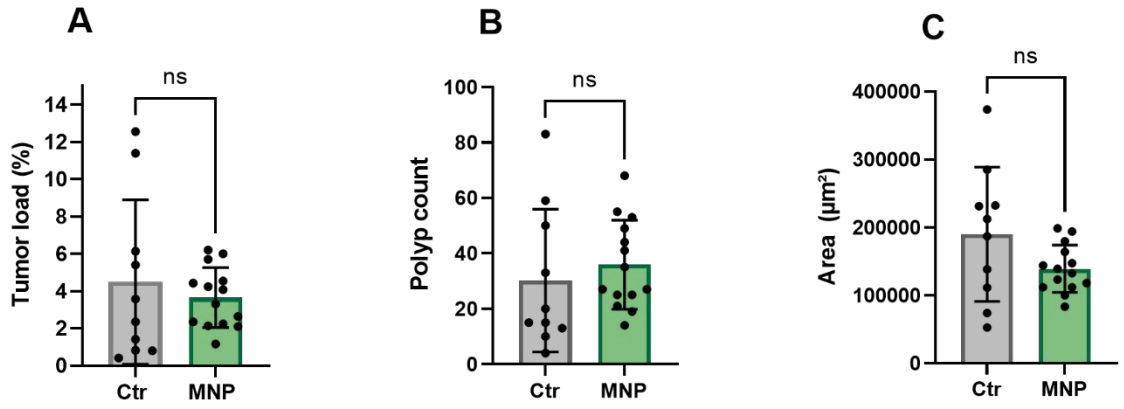

Figure 10: Intestinal polyp analysis of 100-day experiment. Tumour load (A) was analysed using a Mann-Whitney test, whereas polyp count (B) and average polyp area (C) were analysed with a Shapiro-Wilk test. Neither of the parameters showed significant differences.

In addition to quantitative intestinal polyp assessment, lesion severity was evaluated by histopathological grading performed with the support of an expert pathologist. Grading

was based on morphological and structural characteristics of the polyps. The scoring system (for details see section 3.8.2) consisted of 3 levels - low grade, high grade and invasive polyps. The first two levels comprised the majority of detected polyps. Invasive carcinomas were only observed in 4 mice (2 from MNP ♀ and 1 from Ctr ♂ and MNP ♂ each). As different gradings were observed in female and male mice, detailed sex specific grouping is shown in Figure 11.

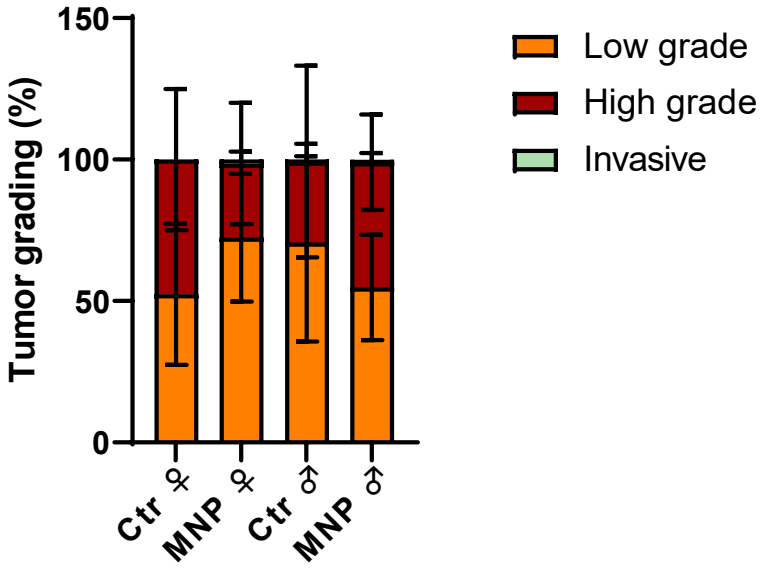

Figure 11: 100-day experiment polyp grading results shown for all four treatment groups. Bars indicate relative proportion of polyps within each severity grade, expressed as a percentage of the total polyp count.

A contradictory trend for different sexes was observed. MNP-treated female mice appeared to have more low-grade polyps and less high-grade polyps than Ctr female mice, whereas males display opposite results. However, mixed-effects model (REML) statistical analysis resulted in absence of significance ($p = 0.0911$) for MNP-treatment and sex interaction. Also separated sex specific analysis did not reveal any significant changes regarding polyp gradings with MNP treatment.

In the H&E stainings also no evident morphological differences were identified between MNP-treated and Ctr mice (Figure 12). Nuclear size, cellular structure and luminal morphology were comparable amongst both treatment groups.

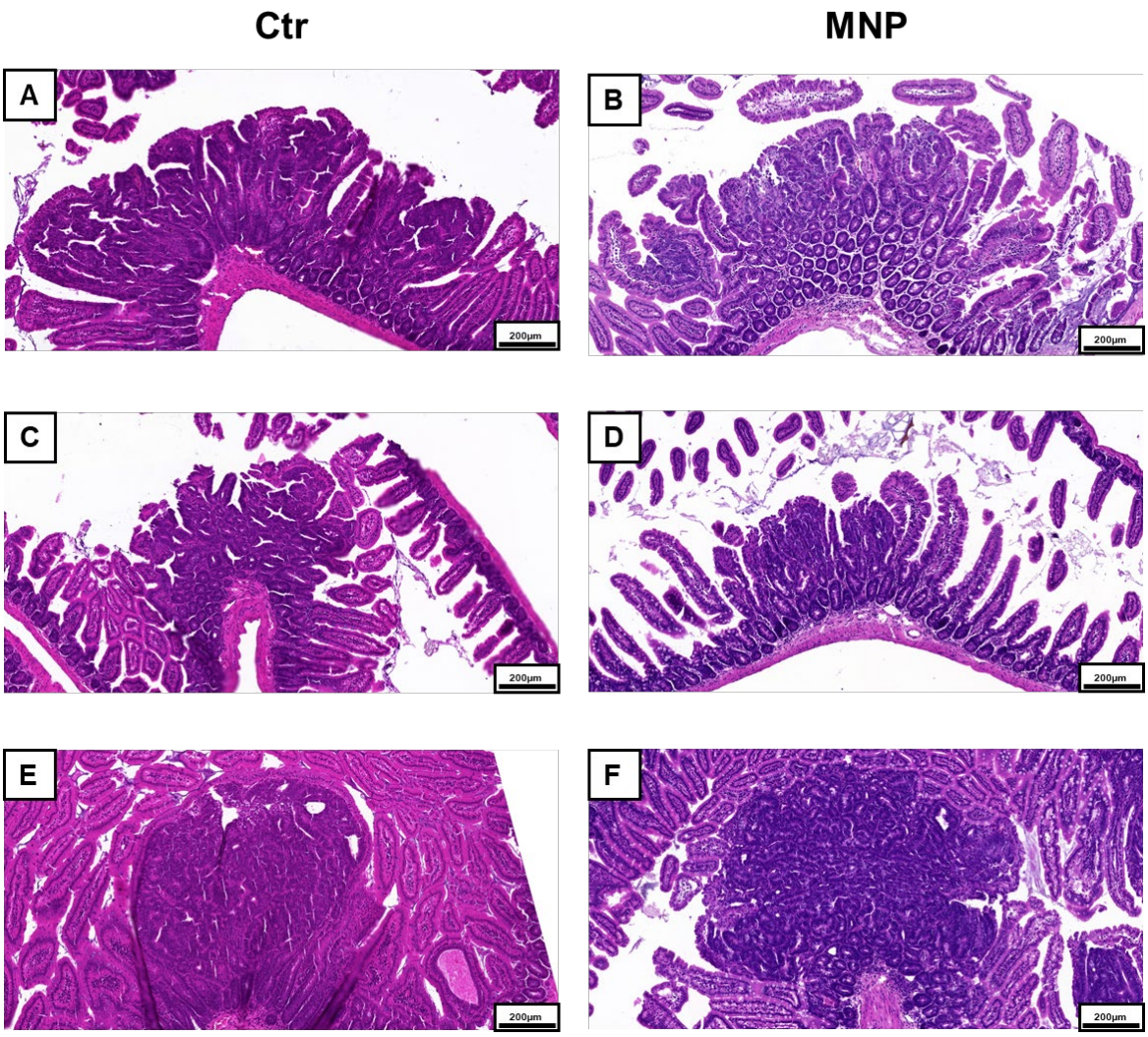

Figure 12: Visual comparison of H&E-stained intestinal polyp morphology between Ctrl (left) and MNP-treated (right) mice.

Minor differences in colour intensity between the two treatment groups can be explained by the fact, that samples were stained manually and respective groups were stained separately. Therefore, differences in staining intensity cannot be interpreted as biologically relevant.

4.2. Survival Experiment

4.2.1. Survival overview using Kaplan-Meier curves

In addition to the 100-day endpoint experiment, a survival experiment was performed to more accurately evaluate how long-term exposure to MNP influenced intestinal neoplasia progression and overall survival. An average lifespan of 120 days for $APC^{Min/+}$ mice raised on a high-fat diet has been reported by Moser et al., 1990.

For this experiment a total of 35 APC$^{Min/+}$ mice (19 females and 16 males) were assigned to two treatment groups (details for grouping see Materials & Methods section 3.3.2, Table 4). In contrast to the 100-day experiment, that had a predefined common endpoint for all subjects, the survival experiment was based on individual endpoints for each subject. Survival time was defined as the interval between the time of birth and the timepoint of humane euthanasia (or actual death). Respective endpoint criteria for humane euthanasia were chosen in order to prevent excessive suffering of the mice (see scoring table in Materials & Methods section 3.4.2, Table 5). Ctr groups received normal corn-based mouse feed, while MNP-treated groups received corn-based mouse feed supplemented with 0.3 mg/MNP-mix (equal parts of previously mentioned MNP types) per 1 g feed. At the beginning of the MNP-food intervention mice were aged between 6 to 13 weeks. Previously mentioned variation in age reflects the logistical challenges in breeding and collecting a sufficient number of APC$^{Min/+}$ mice from sequentially born litters required for the survival study. This also resulted in MNP-treated mice to be exposed to nano- and microplastics for a different percentual part of their life. Of all 35 experimental subjects only four were not prematurely euthanised, but died naturally (one mouse was not eligible for necropsy due to already decomposing organs). Days of survival were documented and analysed. A graphical survival representation was created with Kaplan-Meier curves comparing treatment groups for both sexes separately (Figure 13).

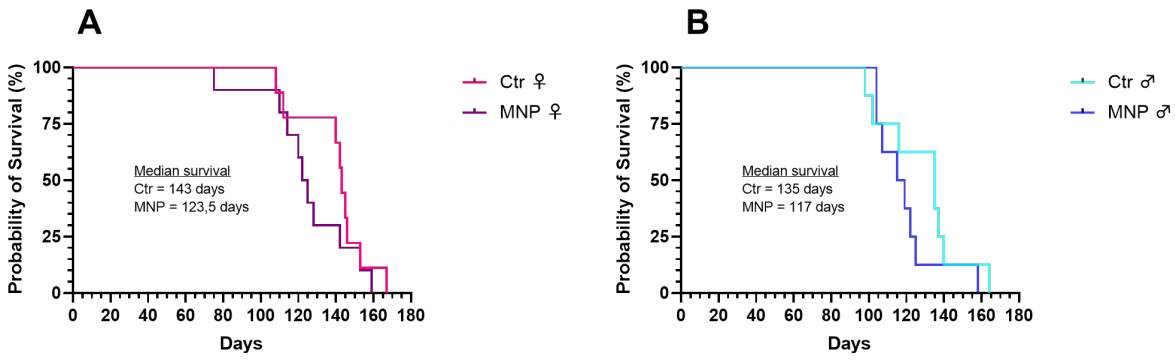

Figure 13: Kaplan-Meier curves and median survival rate comparing MNP-treatment and Ctr groups in females (A) and males (B).

The median survival rate for female APC$^{Min/+}$ mice was 143 days for the Ctr group and 123.5 days for the MNP-treated group. On the other hand, male Ctr mice had a median survival rate of 135 days, while for MNP-treated mice it was just 117 days. Female mice showed on average a higher median survival rate than males (8 days more in Ctr group and 6.5 days

more in MNP group), whereas mice from the Ctr group generally displayed a slightly higher median overall survival than the MNP-treated group (19.5 days for females and 18 days for males).

A statistical analysis of the survival days (male and females combined) was carried out comparing the two treatment groups. Although mean overall survival was decreased with MNP treatment (122.3 days vs 134.3 in Ctr) unpaired t-test with Welch´s correction did not reach statistical significance (p =0.0960) as shown in Figure 14.

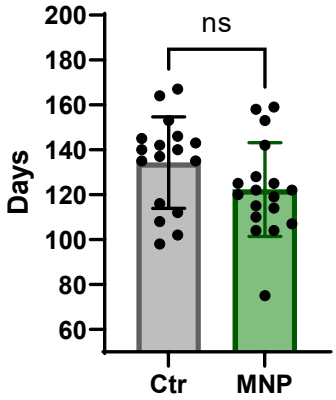

Figure 14: Graphical comparison of overall days of survival for Ctr and MNP-treated groups.

4.2.2. Longitudinal body weight comparison

Because of logistical reasons, $APC^{Min/+}$ mice varied significantly in age when the experiment started. Because of this, their body weight documentation was initiated at different stages of their life and also animals ceased at individual timepoints. A graphical comparison is shown in Figure 15 separately for both sexes. Female mice display a slightly more clustered weight development trajectory than males.

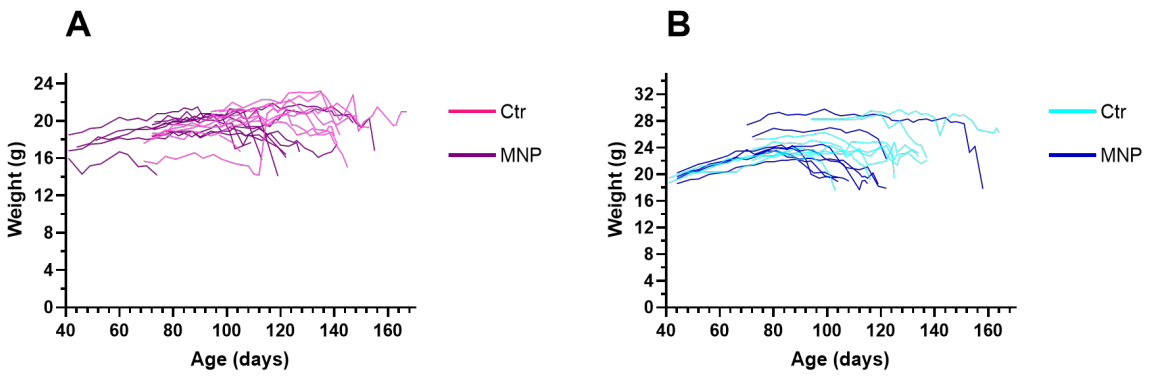

Figure 15: Graphical illustration of body weight development for female (A) and male (B) APC$^{Min/+}$ mice. Each line represents a respective mouse weight development over the experimental timecourse.

On the whole, similarly to the 100-days experiment, no notable differences in body weight development between the two treatment groups can be recognised neither for males, nor for females.

4.2.3. Spleen weight assessment

Consistent with the initial 100-day experiment, spleen weight was additionally analysed in the survival experiment as a secondary lymphoid organ–associated endpoint. This parameter shed light on possible systemic immune-related changes, that can happen during MNP exposure. Spleen samples were collected and the weight documented from 31 of 35 total experimental subjects. A statistical analysis was carried out based on treatment group. A mean spleen weight of 0.3826 g and 0.2616 g was calculated for the Ctr and MNP groups respectively indicating a clearly increased overall spleen weight compared to normal weights reported for adult C57Bl/6J wildtype mice (0.08-0.12 g) (Shepherd et al., 2020). Ctr group mice had significantly heavier ($p = 0.0101$) spleens, than MNP-treated mice (Figure 16). This could be either linked to longer survival, and thus probably more severe anaemia and resulting splenomegaly as a compensatory mechanism (Ren et al., 2019; Shepherd et al., 2020). Alternatively, it could suggest that specific immune cells 'stored' in the spleen might be released by an inflammatory trigger (MNP) and thus serve as an indicator of increased systemic inflammation (Bruno et al., 2024; Z. Zhang et al., 2024). However, spleen weight alone does not allow identification of an underlying pathological mechanism in this case.

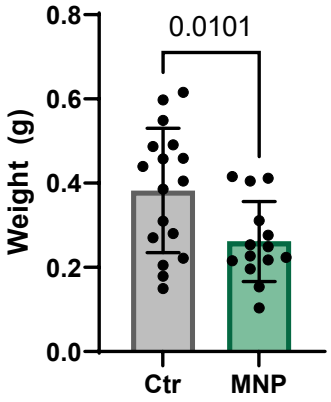

Figure 16: Spleen weight difference between treatment groups. The Ctr group exhibits significantly heavier spleens than MNP-treated mice.

4.2.4. Small intestine polyp burden

To investigate the potential impact of prolonged MNP exposure on intestinal neoplasia progression, polyp burden was evaluated in the survival experiment and compared as for the 100-day endpoint study, in which animals were humanely euthanized at 100 days of age. The procedures for sample preparation, image analysis, and histopathological evaluation with regards to intestinal polyp assessment and scoring were identical to those applied in the 100-day experiment (4.1.3). Small intestine sections of 28 $APC^{Min/+}$ mice (14 Ctr and 14 MNP-treated) were stained with H&E, scanned and analysed via QuPath. for tumour load, average polyp area and polyp count.

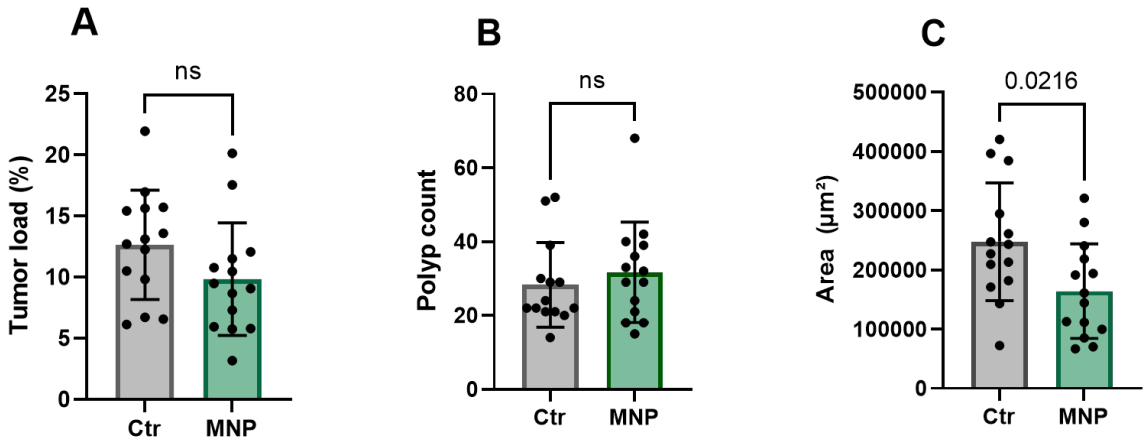

Figure 17. Intestinal polyp analysis of the survival experiment. A Welch´s unpaired t-test was performed for the statistical analysis of tumour load and average polyp are, whereas polyp count was analysed using a Mann-Whitneys t-test. Tumour load (A) and polyp count (B) displayed no significant differences between Ctr and MNP treatment groups Average polyp area (C) is shown to be significantly higher in Ctr mice.

Tumour load showed no significant differences (p = 0.1137) between Ctr and MNP-treated mice, although, similarly to the initial 100-day experiment results, the mean overall tumour load seemed to be decreased in MNP-treated mice as shown in Figure 17, A. Polyp count was not significantly changed (p = 0.4741) (Figure 17, B**).** On the contrary, statistical analysis, regarding average polyp area, displayed significant differences (p = 0.0216) for MNP-treated mice (mean area = 164 101 μm^2) having smaller average polyp area than Ctr mice (mean area = 247 523 μm^2) (Figure 17, C). A similar, albeit unsignificant, tendency was observed in the previous experiment as well. Overall speaking, tumour load, polyp count and average polyp are interconnected, as tumour load is dependent on polyp count and average size. Thus, we observe with significantly decreased average polyp size also a trend of reduced tumour load, however this parameter did not reach statistical significance. On the whole, similar trends regarding polyp burden analysis were noticed in both experimental runs, but seemed to be more pronounced and statistically significant at terminal endpoint of this model.

For polyp scoring, the same grading criteria as described in section 3.8.2. were used.

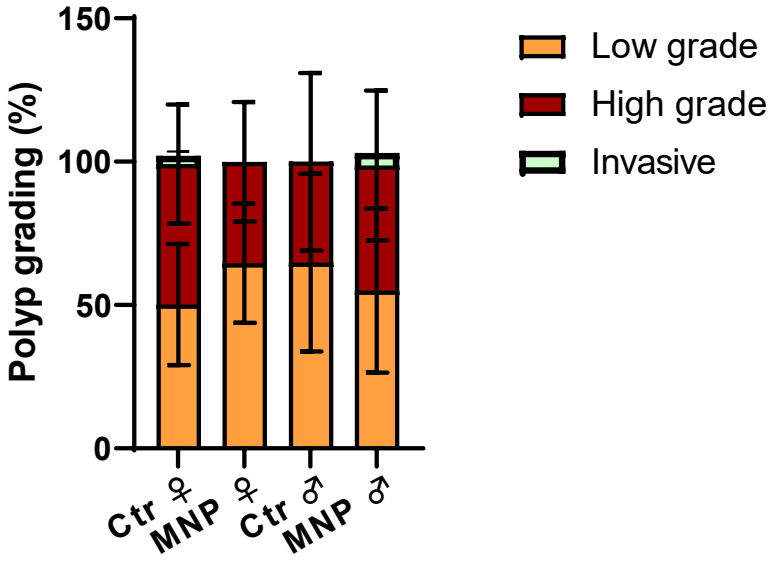

Figure 18. Survival experiment polyp grading results shown for all four treatment groups. Bars indicate relative proportion of polyps within each severity grade, expressed as a percentage of the total polyp count. Statistical analysis was performed using a Two-way-ANOVA.

Statistical analysis showed no significant differences (p = 0.7212) between the experimental groups (Figure 18). However, similarly to the initial 100-day experiment, a trend for sex-specific differences in polyp grading distribution was observed. MNP-treated females

exhibited a shift toward a higher number of low-grade polyps and fewer high-grade polys compared with Ctr female mice, whereas MNP-treated males displayed the reverse pattern.

4.2.5. Overview of immune cell and inflammatory marker expression

As an additional exploration to the spleen weight analysis regarding possible immunological changes due to MNP exposure we investigated immune cell and inflammatory marker expression. It has been described, that, among others, MNPs activate macrophages and neutrophile infiltration, which are known to be part of the innate immune response (Fan & Ha, 2025). Therefore, immunohistochemical stainings for F4/80, Arg1, iNOS, and neutrophil elastase were performed. F4/80 (Figure 19) was used to evaluate macrophage infiltration, while Arg1 (Figure 20) and iNOS (Figure 21) were included to assess macrophage-associated activation patterns, representing anti- and pro-inflammatory phenotypes, respectively. Neutrophil elastase (Figure 22) was used to identify neutrophil-associated inflammatory responses. Representative immunohistochemically stained small intestinal sections of adenomatous polyps from Ctr mice and MNP-treated mice were descriptively compared. Across the evaluated stainings, positive DAB signal was visible as brown staining against a hematoxylin-counterstained background. Overall, staining patterns appeared broadly comparable between Ctr and MNP-treated samples. No apparent treatment-related differences in staining distribution or intensity were evident by descriptive visual assessment. However, a direct comparison between healthy tissue and adenomatous tissue displayed a noticeably lower macrophage infiltration (F4/80 staining, Figure 20) in polyp regions. Unfortunately, due to staining artefacts from remaining paraffin in the tissue section, no quantitative assessment of respective immune cells in the polyps or small intestine was possible.

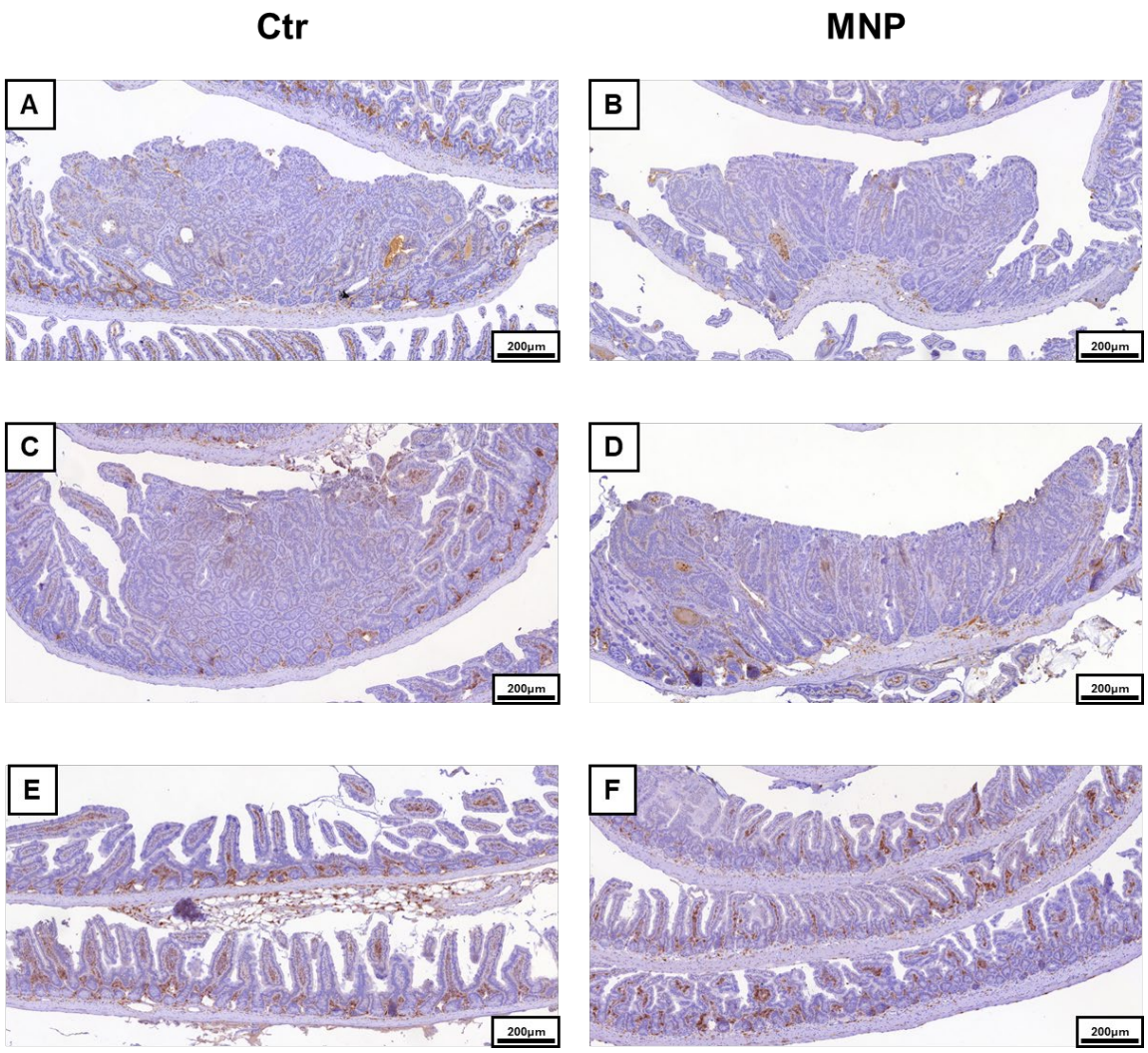

Figure 19: Immunohistochemical staining for F4/80 marker. A 10x amplification of small intestine polyps is shown for the Ctr group (A, C) and MNP-treated group (B, D). For comparison, healthy intestinal tissue is shown for Ctr (E) and MNP (F).

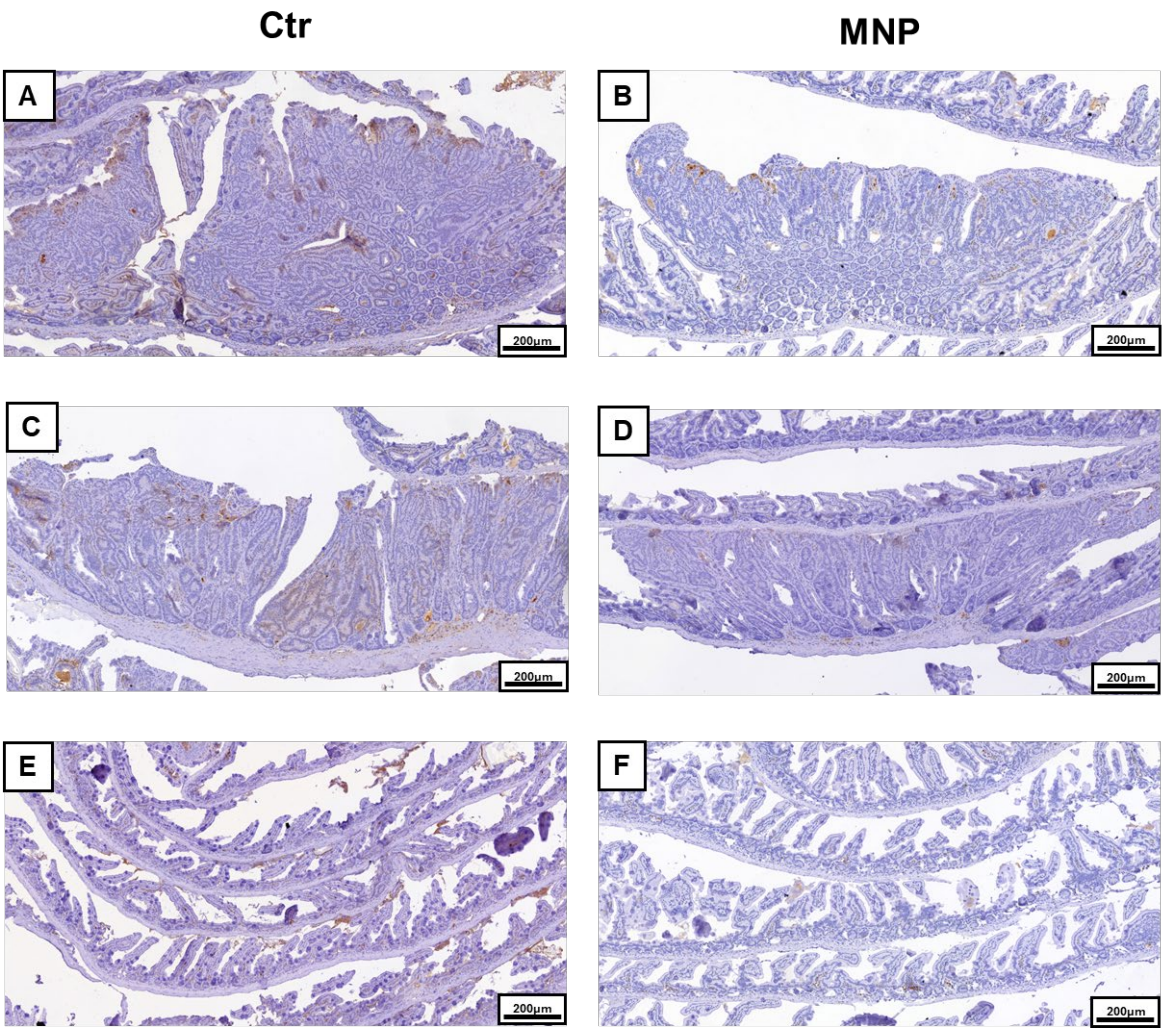

Figure 20: Immunohistochemical staining for Arg1 marker. A 10x amplification of small intestine polyps is shown for the Ctr group (A, C) and MNP-treated group (B, D). For comparison, healthy intestinal tissue is shown for Ctr (E) and MNP (F).

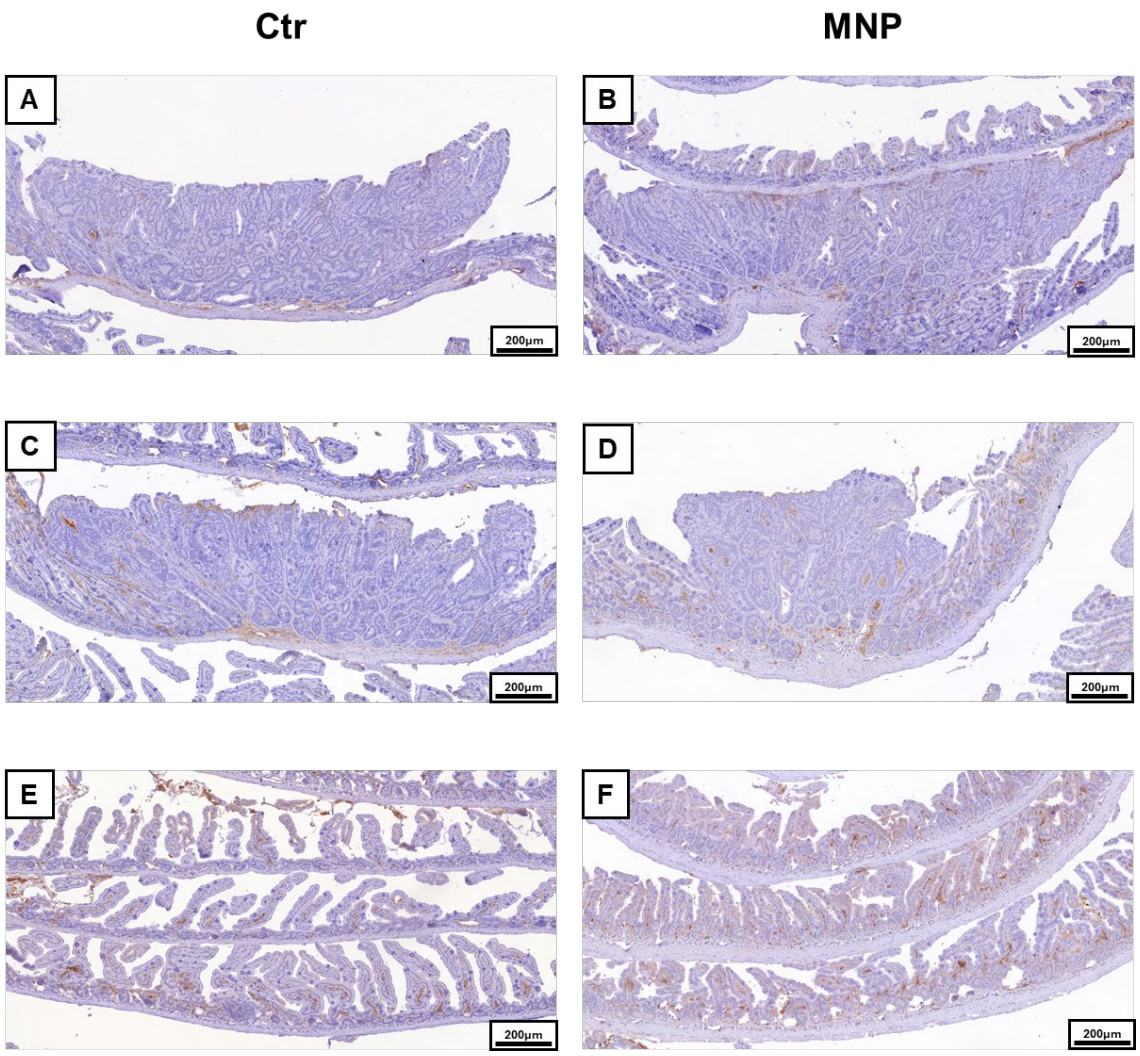

Figure 21: Immunohistochemical staining for iNOS marker. A 10x amplification of small intestine polyps is shown for the Ctr group (A, C) and MNP-treated group (B, D). For comparison, healthy intestinal tissue is shown for Ctr (E) and MNP (F).

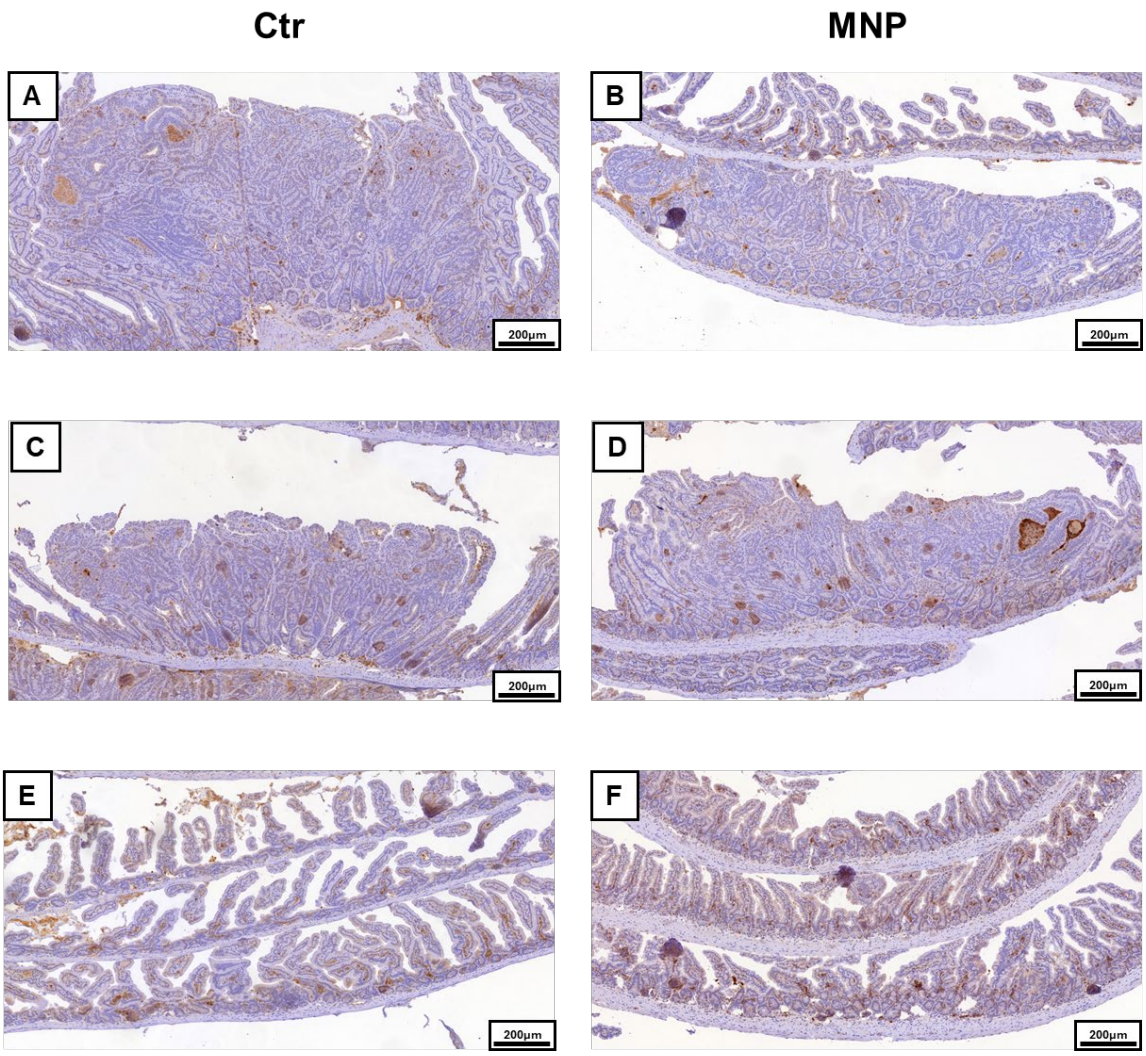

Figure 22: Immunohistochemical staining for neutrophile elastase marker. A 10x amplification of small intestine polyps is shown for the Ctr group (A, C) and MNP-treated group (B, D). For comparison, healthy intestinal tissue is shown for Ctr (E) and MNP (F).

4.2.6. Microscopic visualisation of fluorescent MNPs

In addition to the immunohistochemical staining, fluorescence staining was carried out to assess the localization and distribution of MNP particles in intestinal tissue. Of the three different types of PS MNP particles only the green fluorescent 0.3 µm and red fluorescent 1 µm particles were found in intestinal wall tissue (Figure 23). Particles were sparsely distributed across the whole small intestine, on average around 20 PS particles were found per small intestine section. While multiple particles were identified in healthy intestinal tissue, none were detected in the adenomatous polyps. Some particles were observed in a different plane or on the edge of the tissue, where they might have been displaced during processing or staining. It is also likely, that a part of these PS fluorescent particles was

washed away during excessive washing and deparaffinisation steps, thus no quantitative data is given here.

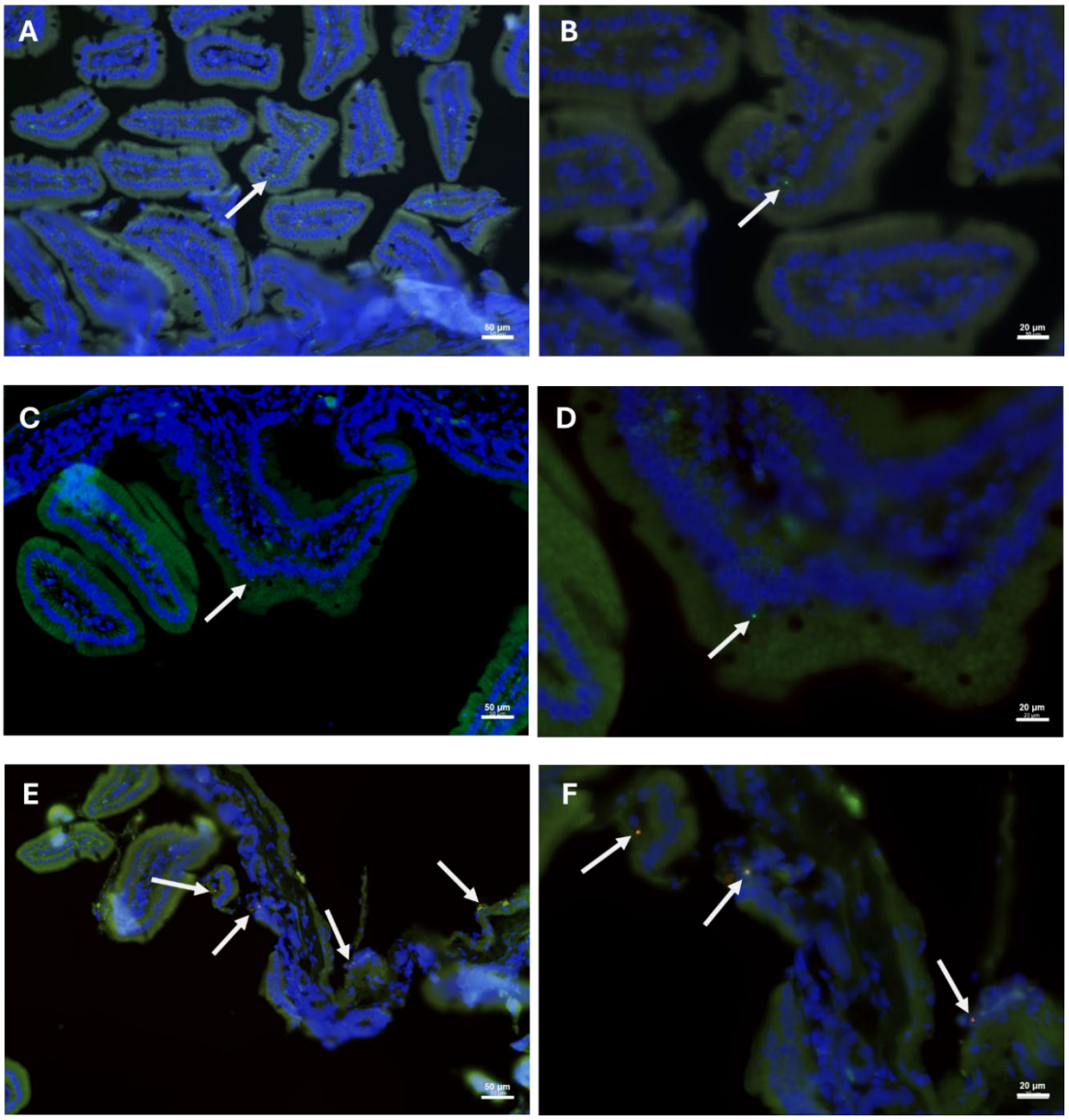

Figure 23. Images of fluorescently stained intestinal wall tissue of an MNP-treated mouse. Arrows point at fluorescently labelled PS MNP particles. On the left the images (A, C, E) are amplified at a 10x rate, whereas on the right side respective 20x amplifications (B, D, F) of said images can be seen. 0.3 µm green fluorescent PS plastic particles are illustrated in images A, B, C, D. 1 µm red fluorescent PS particles can be spotted in images E and F.

5. Discussion

Adenomas represent the classic precursor of CRC, with around 85–90% of sporadic CRCs evolving from adenomas. Yet, less than 10% of adenomas progress to CRC (Conteduca et al., 2013). The molecular mechanism behind human FAP disorder is similar to that of $APC^{Min/+}$ mice (Moser et al., 1995). Concurrently, a number of effects of MNPs on intestinal tissue have been investigated. They include oxidative stress, intestinal barrier dysfunction (Liang et al., 2021; Zeng et al., 2024), gut barrier disruption(Bruno et al., 2024), induction of metabolic changes (Bonanomi et al., 2022) and platelet activation(Bruno et al., 2024). The previously mentioned genetic $APC^{Min/+}$ mouse model was specifically chosen for the purpose of this study, which aimed at investigating MNPs effect on intestinal neoplasia progression.

Two long-term experimental runs – 100-day experiment and survival experiment – were conducted with 25 (15 females and 10 males; exposure starting at 3 to 6 weeks of age) and 35 (19 females and 16 males; exposure starting at 6 to 13 weeks of age) $APC^{Min/+}$ mice respectively. Two treatment groups were formed. Ctr groups received normal corn-based mouse food, while MNP-treated groups received corn-based mouse feed supplemented with 0.3 mg MNP-mix (3 different sizes at equal weight) per 1 g feed.

5.1. Systemic and clinical effects of MNP exposure

Inspection of general health status and weight of individual mice from both treatment groups was a vital task during both experimental runs. Together with terminal end weight, overall survival time and spleen weight at necropsy, these parameters were assessed for both treatment groups to get an idea about the systemic and clinical overall effects of MNP exposure.

During both experimental runs, clinical status of each mouse was visually inspected and body weight documented 3 to 7 times per week. The collected body weight data were then analysed and compared for each sex separately (given that males biologically tend to be heavier than females) between the treatment groups. No statistically significant difference was detected between treatment groups for both sexes. In both experimental runs – 100 days and survival - mice showed almost identical body weight development trajectory. Sex-

specific end weight comparison of the 100-day experiment similarly showed no statistically significant differences between treatment groups, which overall indicates that MNP application in food was well tolerated by the mice and lead to no notable changes in weight gain as well as endpoint weight. Also, mice did not observe any major physical or health related distress by MNP application, which would result in less food uptake or reduced body weight up to the 100-day timepoint. These results go in accordance with similar studies, which found that consumption of ~ 80 µg/kg/day of 1 µm PS MNPs via drinking water for 8 weeks led to no noticeable weight loss in C57BL/6J mice (Rawle et al., 2022). A different study from Zhang et al., 2024 also detected no significant body weight difference in wildtype mice, who received an orally gavaged dose of 0.5 mg of 0.5 µm PS plastic particles in 100 µl sterile deionized water once a day for 8 weeks. However, mice from the same experiment, which had consumed larger plastic particles (5 µm), had an increased body weight, which might hint at a size-dependant effect (Z. Zhang et al., 2024).

The main clinical assessment of the survival experiment, was the overall survival rate. Some scientific sources report, that on average $APC^{Min/+}$ mice survive around 120 days (Boivin et al., 2003; Moser et al., 1995), whereas others describe an average lifespan of this genetic mouse model to be between 120 and 150 days (Ren et al., 2019).

Collected data (days of survival) from the survival experiment yielded no significant results regarding treatment group differences ($p = 0.0960$), however a tendency for slightly lower mean survival time was observed in the MNP-treated group (122.3 days) versus Ctr group (134.3 days). This difference was insufficient for statistical significance most probably due to a big variation in mouse age at the beginning of the experiment, as well as possible sex specific effects, such as the carcinogenic effect of male hormones described by Amos-Landgraf et al., 2014.

$APC^{Min/+}$ mice have in general a low life expectancy due to side effects of the genetic mutation, such as multiple intestinal adenoma development, intestinal bleeding and successive chronic anaemia (Ren et al., 2019). It has been shown, that MNPs can induce multiple immunological and inflammatory pathways (Fan & Ha, 2025), which might lead to an increased intestinal barrier dysfunction and inflammation (Ren et al., 2019; Shepherd et al., 2020; Wang et al., 2023) which could in turn also aggravate intestinal tumorigenesis.

Li et al. has described inflammation as a common promotor of colon tumorigenesis (Li et al., 2022).

Moreover, spleen weight analysis was conducted for both long-term experiments. Results for the 100-day experiment showed no statistical significance ($p = 0.3154$) between MNP and Ctr mice at this timepoint, whereas spleen weight in the survival experiment was significantly lower in MNP-treated mice ($p = 0.0101$). This might be due to the fact, that MNPs induced immunological pathways (Fan & Ha, 2025) early on in the MNP-treated group, which led to a more rapid tumour suppression, than in the Ctr group and thus a lower weight later-on. As $APC^{Min/+}$ mice develop chronic anaemia and intestinal polyps throughout their life, this result might not be entirely accurate as immunological responses in $APC^{Min/+}$ mice would be induced early in their life (Shepherd et al., 2020) and thus might mask possible ensuing immunological effects of MNPs.

Although some parameters showed significance (spleen weight) or insignificant sex-specific survival trends (females > males), further analysis with bigger experimental groups are needed. The variations and specific tendencies e.g. overall survival time might have been skewed by gender effects or due to different mouse litters, heterogeneity of the genetic mouse model or age (6 to 13 weeks) at the start of the survival experiment.

5.2. Effects of MNP exposure on intestinal tumour development

After reaching experimental endpoint – either at 100 days of age or at humane endpoint in survival experiment - mice were dissected, organs collected and processed, and small intestine was sectioned and stained for histopathological assessment.

Tumour load, average polyp area, polyp count and general polyp scoring were assessed from H&E stains. Polyp counts showed no statistically significant differences between treatment groups in both experiments and mean values ranged between ~ 28-37 polyps per small intestine in both experiments, meaning that the same amount of polyps was present at 100 day timepoint as well as at the end of life. Tumour load was also not statistically significant for both experiments when comparing treatment groups, however a slightly reduced overall tumour load ($p = 0.1137$) was observed for the MNP group (mean value at 9.84%) in the survival experiment compared to the Ctr group (mean value at 12.65%). Of note, overall tumour load was at only 3-4% at 100 days timepoint compared to 10-12.6% at

the end of life indicating a major increase in size of already established polyps during that time.

Average polyp area, on the other hand, showed statistically significant differences ($p = 0.0216$) between treatment groups in the survival experiment, indicating an around 34% lower average polyp area in MNP-treated mice (164 101 μm^2) when compared to Ctr mice (247 523 μm^2). Moreover, albeit statistically insignificant ($p = 0.0885$), a similar tendency toward slightly lower average polyp area values in MNP-treated mice (139 325 μm^2) compared to Ctr (189 987 μm^2) mice was also displayed in the 100-day experiment.

It has been established, that MNPs induce a variety of immunological responses, one of which is the activation of NF-κB signalling (Fan & Ha, 2025). NF-κB in turn activates COX-2, as an initial response to cellular stress, which is then reported to lead to reduction of small intestine polyp size and number (Ren et al., 2019). This information might support the reduced average polyp size in MNP-treated groups, when compared to Ctr groups. In addition, tumour load exhibits a positive correlation with average polyp area, which means, that MNP-treated groups had significantly smaller intestinal polyps and a trend of also lower tumour load than Ctr groups at constant polyp numbers. This might be a result of a timely MNP-induced immune response, which led to a shrinkage or slower growth of mentioned polyps.

Furthermore, analytical results from intestinal polyp grading exhibited no statistically significant differences between the treatment groups in neither of the experimental runs. Polyp stages were mostly low grade and high grade and almost equally balanced with a slight tendency towards more low-grade polyps in both experimental runs. Invasive carcinomas were only observed in 6 mice total. Nonetheless, in both the 100-day experiment and survival experiment MNP-treated female mice appeared to have more low-grade polyps and less high-grade polyps than Ctr female mice, whereas males displayed opposite results. A study done by Amos-Landgraf et al. on mice, who used a chemically induced carcinogenesis mouse model, found, that male hormones promote adenoma formation (Amos-Landgraf et al., 2014). This could implicate, that instead of possible MNP-induced early immunological responses and subsequent tumour reduction, there´s an add-on effect to the tumorigenic testosterone effect in male mice, which might explain a potential shift towards higher numbers of high-grade polyps in males.

Overall, it would be suggested to repeat the long-term experiments, specifically the survival experiment, with a bigger experimental batch, in order to minimise sex-related variations, avoid batch effect and reduce the impact of the heterogeneity of $APC^{Min/+}$ mouse model. Some studies found, that intestinal polyp formation is highly dependent on genetic background and variations, as well as sex-dependant metabolic and molecular differences (Dorman et al., 2021; Wang et al., 2023). A higher experimental subject number would help to gather more robust data and lessen the impact of breeding variations and sex-specific effects in the $APC^{Min/+}$ mouse model. This might help strengthen and back-up the statistically significant data regarding MNPs effect on average polyp area and might simultaneously help investigate the tendencies mentioned for tumour load and polyp scoring.

5.3. Immunological and fluorescent characterization of tissue responses

$APC^{Min/+}$ mouse model is well known for its intestinal polyp formation. Even though polyp initiation is mainly driven by a genetic nonsense mutation, other mechanisms are considered to influence polyp growth and potential tumour progression. One of these mechanisms is immunological activity (Ren et al., 2019). MNPs are known to activate first-line macrophages and neutrophils (Fan & Ha, 2025), which produce reactive oxygen species and reactive nitrogen intermediates, which in turn might damage epithelial DNA and contribute to further mutagenesis (Grivennikov, 2013).

Immunological staining was done with F4/80, Arg1, iNOS and neutrophile elastase for the survival experiment, with the purpose to investigate immune cell (macrophage and neutrophile) activity and infiltration in intestinal tissue, especially in adenomatous polyps. Unfortunately, due to paraffin residues and staining artefacts, only a qualitative descriptive analysis was possible, but not a quantitative.

In general, there were no visible differences observed in the amounts or location of macrophage (F4/80) or neutrophile (neutrophile elastase) immune cell infiltration between Ctr and MNP groups. Also pro-(iNOS) and anti-(Arg1)inflammatory macrophage levels were similar among treatment groups. Intestinal polyps displayed a relatively low number of immune cells present in all four staining types in both treatment groups. However, the

F4/80 staining, which demonstrates macrophage infiltration, had visibly fewer immune cells in adenomatous tissue compared to healthy intestinal tissue for both Ctr and MNP-treated mice. Overall, there were no apparent differences in immune cell presence and infiltration between the two treatment groups. Also another study has found, that small intestine adenomatous tissue exhibited a visibly lower conventional T- cell and B-cell infiltration and a higher Treg (regulatory T-cell) accumulation in comparison to healthy intestinal tissue (Akeus et al., 2014). This might hint at an altered immune setting at early-stage adenoma development and explain the lower number of positive immune cells displayed in intestinal polyps, compared with healthy tissue in the survival experiment.

Furthermore, fluorescence staining of tissues was performed in order to assess MNP distribution across the small intestine. After analysing the fluorescently stained samples, a relatively low number of fluorescently labelled PS MNPs was detected in the small intestine section. Moreover, these PS particles were mainly observed in or latched on healthy intestinal tissue. No fluorescent PS particles were found in intestinal polyps. This sparce number of plastic particles might be a result of washing-out after numerous tissue processing steps, however a study conducted by Kopatz et al., which researched MNP uptake (0.9 mg/day MNP mix) in a colitis mouse model also observed generally low numbers of MNPs in intestinal tissue after a 10 day experimental run. Thus indicating that MNP levels directly in the small intestinal tissue might be generally low and particles do not tend to accumulate in higher numbers in intestinal epithelium (Kopatz et al., 2025).

5.4. Study limitations

Despite meticulous planning of both experimental runs, certain inconsistencies were inevitable. One of these deviations was the age difference of $APC^{Min/+}$ mice at the start of both experiments. Mice were aged 3 to 6 weeks at the start of the 100-day experiment and 6 to 13 weeks at the start of survival experiment. This difference was unavoidable, as multiple breeding pairs were needed to achieve sufficient amounts of mice and females did not give birth simultaneously. Both experiments had to be performed in at least two separate experimental runs in order to collect a sufficient experimental batch of $APC^{Min/+}$ mice.

Due to the difference in age at the start of both experimental runs, mice were exposed to MNPs for a different period of their individual life. Additionally, due to breeding irregularities, the batch effect of the different mouse litters was stronger, whereas the heterogeneity of the genetic mouse model most probably also played a role in varying results.

Moreover, fluorescently labelled PS particles, that were used in the experiments, were industrially-produced and, perfectly round spheres. These particles were chosen because a subsequent detection with a fluorescent microscope was planned. The disadvantage was however, that these particles most probably do not represent "real-to-life" plastics that are found in the environment (Yong et al., 2020).

In addition, as to avoid extensive contamination of laboratory equipment and Ctr subjects with MNPs treatment groups, Ctr were handled and weighed before MNP-treated groups and all following sample processing steps starting with mouse dissection and ending with tissue staining and mounting, were carried out for both treatment groups separately. This could have led to particular batch effects, such as difference in tissue staining intensity. However, this had little impact on the descriptive analysis, that was performed in our case.

6. Conclusion

The main aim of this study, was to investigate possible effects of MNP on intestinal neoplasia progression. Intestinal tumour assessment and analysis yielded meaningful results in both experimental groups with average polyp area initially (100-day experiment) showing a trend towards and then a statistically significantly (survival experiment) lower area in MNP-treated mice. The remaining parameters (polyp count, tumour load and polyp grading) displayed no statistically significant differences between the treatment groups. These results might indicate, that MNPs reduce average polyp area and thus halt intestinal tumour development. However, the clear mechanism – potentially via MNP activation of immune cells or direct MNP inhibitory effects on polyp growth – still needs to be elucidated.

Additionally, physiological parameters were also compared between treatment groups in both experiments. Body weight progression and end-weight comparison between the two treatment groups in both experimental runs were identical. This suggested, that MNPs in mouse food were well tolerated and had no discernible adverse effects up to day 100 of age. Spleen weight was another parameter, that was investigated and showed to be statistically significantly lower in MNP-treated mice in the survival experiment. This might hint at MNPs inducing immune cell infiltration in intestinal tissue early-on, at the initiation of adenoma formation. This could subsequently have an impact on and explain the significantly lower average polyp area.

Overall survival comparison between the treatment groups showed a trend for lower survival in MNP-treated mice, however it did not reach statistical significance potentially also due to sex specific different observations and low group numbers when analysing each sex separately. Contrarily to the lower polyp size in this group, other factors may have reduced survival time in the MNP-treated group, such as MNP-induced inflammation or intestinal barrier disruption.

Finally, an immunological analysis showed no differences between the treatment groups. Among all four immunological stainings – F4/80, Arg1, iNOS and neutrophil elastase – the number of detected immune cells was highly comparable between both treatment groups. It was also noticed, that immune cell presence was scarce in intestinal adenomatous

formations compared to healthy adjacent tissue. This could indicate, that immune cell infiltration had taken place at an earlier stage, e.g. with MNP-treatment earlier, than without. Because of this, intestinal polyp development might have been halted in MNP-treated mice earlier than in Ctr mice, therefore leading to smaller average polyp size in the MNP-group.

To conclude, although most of the conducted analysis showed no statistical significance, average polyp area and spleen weight were significantly lower in MNP-treated mice. MNP-treated mice also displayed a trend towards lower overall survival compared to their Ctr counterparts. These results indicate, that MNPs might reduce intestinal polyp size, perhaps through early immune system activation leading to reduced growth rate of polyps. Additionally, MNPs might also cause a more severe intestinal inflammation and thus contribute to a shorter life expectancy.

These findings indicate, that MNPs might have surprisingly under certain circumstances a rather positive effect on tumorigenesis in the context of already established polyps, as MNP particles were shown to significantly reduce intestinal polyp size. This might also lead to a reduced tumour progression to invasive carcinomas and thus a decreased risk of CRC development, which would lead to an improved clinical outcome. However, also negative effects were observed on overall survival of APC^{Min+} mice, caused probably by increased inflammation by MNPs early-on.

Due to this, a more thorough analysis of MNP effects on intestinal neoplasia is required to exactly understand the underlying mechanism that MNP exposure triggers in this model. A repetition of the long-term experiments with a higher number of mice and a repetitive analysis of average tumour area, tumour load, polyp count and general polyp scoring would be beneficial, as to confirm or challenge obtained results. An immune cell examination in the splenic tissue, as well as other organs would also be of interest, as to determine the extent of possible immune response. An additional quantitative study examining the immune cell infiltration in healthy and neoplastic intestinal tissue at different mouse development stages would help determine, if MNPs induce an immune response early-on and how this might affect tumorigenesis and overall survival.

In summary, MNPs have shown to have a surprisingly positive effect in reducing intestinal polyp size and could thus, under certain circumstances, be implemented for cancer therapy. However, this might prove to be only true for already established benign polyps, as it was the case in this genetic model of $APC^{Min/+}$ mice. Thus, the effects of long-term chronic MNP exposure on tumour initiation or progression of malignant lesions needs to be evaluated. More detailed research in this context is needed to determine the mechanism behind these findings and to investigate potential side-effects.

List of Abbreviations

$APC^{Min/+}$	Heterozygous mutation in adenomatous polyposis coli (APC) gene, multiple intestinal neoplasia (Min) allele
CRC	Colorectal cancer
Ctr	Control
DAB	3.3′-diaminobenzidine
DNA	Deoxyribonucleic acid
dNTP	Deoxynucleoside triphosphate
DEPC	Diethylpyrocarbonate
FAP	Familial adenomatous polyposis
HindIII	Type II restriction endonuclease isolated from Haemophilus influenzae
IL	Interleukin
KRAS	Kirsten rat sarcoma virus oncogene homologue
MNP	Micro- and nanoplastic
PBS	Phosphate-buffered saline
PCR	Polymerase chain reaction
PFA	Paraformaldehyde
PS	Polystyrene
REML	Restricted maximum likelihood
rpm	Rotations per minute
TAE	Tris-acetate-EDTA
TBS-T	Tris-buffered saline with Tween® 20
TP53	Tumour protein 53
Wnt	Wingless-related integration site
TCF	T-cell factor

List of Tables

List of Supplementary Tables

List of Figures

List of Supplementary Figures

7. References

Akeus, P., Langenes, V., Von Mentzer, A., Yrlid, U., Sjöling, Å., Saksena, P., Raghavan, S., & Quiding-Järbrink, M. (2014). Altered chemokine production and accumulation of regulatory T cells in intestinal adenomas of APC(Min/+) mice. *Cancer Immunology, Immunotherapy: CII*, *63*(8), 807–819. https://doi.org/10.1007/S00262-014-1555-6

Amos-Landgraf, J. M., Heijmans, J., Wielenga, M. C. B., Dunkin, E., Krentz, K. J., Clipson, L., Ederveen, A. G., Groothuis, P. G., Mosselman, S., Muncan, V., Hommes, D. W., Shedlovsky, A., Dove, W. F., & Van Den Brink, G. R. (2014). Sex disparity in colonic adenomagenesis involves promotion by male hormones, not protection by female hormones. *Proceedings of the National Academy of Sciences of the United States of America*, *111*(46), 16514–16519.

https://doi.org/10.1073/PNAS.1323064111/-/DCSUPPLEMENTAL

Aparicio, T., Pachev, A., Laurent-Puig, P., & Svrcek, M. (2022a). Epidemiology, Risk Factors and Diagnosis of Small Bowel Adenocarcinoma. *Cancers*, *14*(9), 2268. https://doi.org/10.3390/CANCERS14092268

Aparicio, T., Zaanan, A., Svrcek, M., Laurent-Puig, P., Carrere, N., Manfredi, S., Locher, C., & Afchain, P. (2014). Small bowel adenocarcinoma: Epidemiology, risk factors, diagnosis and treatment. *Digestive and Liver Disease*, *46*(2), 97–104. https://doi.org/10.1016/j.dld.2013.04.013

Bankhead, P., Loughrey, M. B., Fernández, J. A., Dombrowski, Y., McArt, D. G., Dunne, P. D., McQuaid, S., Gray, R. T., Murray, L. J., Coleman, H. G., James, J. A., Salto-Tellez, M., & Hamilton, P. W. (2017). QuPath: Open source software for digital pathology image analysis. *Scientific Reports 2017 7:1*, *7*(1), 16878-. https://doi.org/10.1038/s41598-017-17204-5

Barker, N., Ridgway, R. A., Van Es, J. H., Van De Wetering, M., Begthel, H., Van Den Born, M., Danenberg, E., Clarke, A. R., Sansom, O. J., & Clevers, H. (2008a). Crypt stem cells as the cells-of-origin of intestinal cancer. *Nature 2008 457:7229*, *457*(7229), 608–611. https://doi.org/10.1038/nature07602

Barnes, D. K. A., Galgani, F., Thompson, R. C., & Barlaz, M. (2009). Accumulation and fragmentation of plastic debris in global environments. *Philosophical Transactions of the Royal Society of London. Series B, Biological Sciences*, *364*(1526), 1985–1998. https://doi.org/10.1098/RSTB.2008.0205

Boivin, G. P., Washington, K., Yang, K., Ward, J. M., Pretlow, T. P., Russell, R., Besselsen, D. G., Godfrey, V. L., Doetschman, T., Dove, W. F., Pitot, H. C., Halberg, R. B., Itzkowltz, S. H., Groden, J., & Coffey, R. J. (2003). Pathology of mouse models of intestinal cancer: Consensus report and recommendations. *Gastroenterology*, *124*(3), 762–777. https://doi.org/10.1053/gast.2003.50094

Bonanomi, M., Salmistraro, N., Porro, D., Pinsino, A., Colangelo, A. M., & Gaglio, D. (2022). Polystyrene micro and nano-particles induce metabolic rewiring in normal human colon cells: A risk factor for human health. *Chemosphere*, *303*, 134947. https://doi.org/10.1016/J.CHEMOSPHERE.2022.134947

Bouvier, A. M., Robaszkiewicz, M., Jooste, V., Cariou, M., Drouillard, A., Bouvier, V., Nousbaum, J. B., Amadeo, B., Arveux, P., Baldi, I., Bara, S., Clavel, J., Colonna, M., Coureau, G., Cowppli-Bony, A., Dabakuyo, S., Dalmeida, T., Daubisse-Marliac, L., Defossez, G., … Woronoff, A. S. (2019). Trends in incidence of small bowel cancer according to histology: a population-based study. *Journal of Gastroenterology 2019 55:2*, *55*(2), 181–188. https://doi.org/10.1007/S00535-019-01636-Z

Bruno, A., Dovizio, M., Milillo, C., Aruffo, E., Pesce, M., Gatta, M., Chiacchiaretta, P., Di Carlo, P., & Ballerini, P. (2024). Orally Ingested Micro- and Nano-Plastics: A Hidden Driver of Inflammatory Bowel Disease and Colorectal Cancer. *Cancers*, *16*(17), 3079. https://doi.org/10.3390/CANCERS16173079

Cetin, M., Demirkaya Miloglu, F., Kilic Baygutalp, N., Ceylan, O., Yildirim, S., Eser, G., & Gul, H. İ. (2023). Higher number of microplastics in tumoral colon tissues from patients with colorectal adenocarcinoma. *Environmental Chemistry Letters 2023 21:2*, *21*(2), 639–646. https://doi.org/10.1007/S10311-022-01560-4

Chamas, A., Moon, H., Zheng, J., Qiu, Y., Tabassum, T., Jang, J. H., Abu-Omar, M., Scott, S. L., & Suh, S. (2020). Degradation Rates of Plastics in the Environment. *ACS Sustainable Chemistry & Engineering*, *8*(9), 3494–3511.

https://doi.org/10.1021/ACSSUSCHEMENG.9B06635

Chen, X., Xuan, Y., Chen, Y., Yang, F., Zhu, M., Xu, J., & Chen, J. (2024). Polystyrene nanoplastics induce intestinal and hepatic inflammation through activation of NF-κB/NLRP3 pathways and related gut-liver axis in mice. *Science of the Total Environment, 935, 173458*. https://doi.org/10.1016/j.scitotenv.2024.173458

Conteduca, V., Sansonno, D., Russi, S., & Dammacco, F. (2013). Precancerous colorectal lesions (Review). *International Journal of Oncology*, *43*(4), 973–984.

https://doi.org/10.3892/IJO.2013.2041

Cox, K. D., Covernton, G. A., Davies, H. L., Dower, J. F., Juanes, F., & Dudas, S. E. (2019). Human Consumption of Microplastics. *Environmental Science & Technology*, *53*(12), 7068–7074. https://doi.org/10.1021/ACS.EST.9B01517

Dick Vethaak, A., & Legler, J. (2021). Microplastics and human health. *Science (New York, N.Y.)*, *371*(6530), 672–674. https://doi.org/10.1126/SCIENCE.ABE5041

Dietrich, W. F., Lander, E. S., Smith, J. S., Moser, A. R., Gould, K. A., Luongo, C., Borenstein, N., & Dove, W. (1993). Genetic identification of Mom-1, a major modifier locus affecting Min-induced intestinal neoplasia in the mouse. *Cell*, *75*(4), 631–639. https://doi.org/10.1016/0092-8674(93)90484-8

Dorman, A., Binenbaum, I., Abu-Toamih Atamni, H. J., Chatziioannou, A., Tomlinson, I., Mott, R., & Iraqi, F. A. (2021). Genetic mapping of novel modifiers for ApcMin induced intestinal polyps' development using the genetic architecture power of the collaborative cross mice. *BMC Genomics, 22, Article 566. (2021), 22*(1). https://doi.org/10.1186/S12864-021-07890-X

Dris, R., Gasperi, J., Mirande, C., Mandin, C., Guerrouache, M., Langlois, V., & Tassin, B. (2017). A first overview of textile fibers, including microplastics, in indoor and outdoor environments. *Environmental Pollution*, *221*, 453–458. https://doi.org/10.1016/J.ENVPOL.2016.12.013

Fan, J., & Ha, Y. (2025). Micro- and Nanoplastics and the Immune System: Mechanistic Insights and Future Directions. *Immuno 2025, Vol. 5, Page 52*, *5*(4), 52. https://doi.org/10.3390/IMMUNO5040052

Fayshal, M. A. (2024). Current practices of plastic waste management, environmental impacts, and potential alternatives for reducing pollution and improving management. *Heliyon*, *10*(23), e40838. https://doi.org/10.1016/J.HELIYON.2024.E40838

Fre, S., Pallavi, S. K., Huyghe, M., Laé, M., Janssen, K. P., Robine, S., Artavanis-Tsakonas, S., & Louvard, D. (2009). Notch and Wnt signals cooperatively control cell proliferation and tumorigenesis in the intestine. *Proceedings of the National Academy of Sciences of the United States of America*, *106*(15), 6309–6314. https://doi.org/10.1073/PNAS.0900427106

Geyer, R., Jambeck, J. R., & Law, K. L. (2017). Production, use, and fate of all plastics ever made. *Science Advances*, *3*(7), e1700782. https://doi.org/10.1126/sciadv.1700782

Gonçalves, C., Martins, M., Costa, M. H., & Costa, P. M. (2018). Development of a method for the detection of polystyrene microplastics in paraffin-embedded histological sections. *Histochemistry and Cell Biology*, *149*(2), 187–191. https://doi.org/10.1007/S00418-017-1613-1

Grivennikov, S. I. (2013). Inflammation and colorectal cancer: colitis-associated neoplasia. *Seminars in Immunopathology*, *35*(2), 229–244. https://doi.org/10.1007/S00281-012-0352-6

Itzkowitz, S. H., & Yio, X. (2004). Inflammation and cancer IV. Colorectal cancer in inflammatory bowel disease: the role of inflammation. *American Journal of Physiology. Gastrointestinal and Liver Physiology*, *287*(1), G7–G17. https://doi.org/10.1152/AJPGI.00079.2004

Jasperson, K. W., Tuohy, T. M., Neklason, D. W., & Burt, R. W. (2010). Hereditary and Familial Colon Cancer. *Gastroenterology*, *138*(6), 2044-2058. https://doi.org/10.1053/J.GASTRO.2010.01.054

Keum, N. N., & Giovannucci, E. (2019). Global burden of colorectal cancer: emerging trends, risk factors and prevention strategies. *Nature Reviews Gastroenterology & Hepatology 2019 16:12*, *16*(12), 713–732. https://doi.org/10.1038/s41575-019-0189-8

Kim, Y. N., Yoon, J. H., & Kim, K. H. (2020). Microplastic contamination in soil environment - A review. *Soil Science Annual*, *71*(4), 300–308. https://doi.org/10.37501/SOILSA/131646

Kopatz, V., Resch, U., Draganic, K., Horvath, A., Pfneissl, J., Kabiljo, J., Mödl, B., Timelthaler, G., Wallner, J., Mirzaei, Z., Beratlyte, S., Schlederer, M., Sarbu, S., Laslau, S., Hollóczki,

O., Raigel, M., Gruber, E. S., Widder, J., Kufferath, I., … Kenner, L. (2025). Polystyrene micro- and nanoplastics in a colitis mouse model – effects on biodistribution, macrophage polarization, and gut microbiome. *Microplastics and Nanoplastics 2025 6:1*, *6*(1), 9. https://doi.org/10.1186/S43591-025-00160-7

Korinek, V., Barker, N., Morin, P. J., Van Wichen, D., De Weger, R., Kinzler, K. W., Vogelstein, B., & Clevers, H. (1997). Constitutive transcriptional activation by a beta-catenin-Tcf complex in APC-/- colon carcinoma. *Science (New York, N.Y.)*, *275*(5307), 1784–1787. https://doi.org/10.1126/SCIENCE.275.5307.1784

Legué, L. M., Bernards, N., Gerritse, S. L., van Oudheusden, T. R., de Hingh, I. H. J. T., Creemers, G. J. M., ten Tije, A. J., & Lemmens, V. E. P. P. (2016). Trends in incidence, treatment and survival of small bowel adenocarcinomas between 1999 and 2013: a population-based study in The Netherlands. *Acta Oncologica (Stockholm, Sweden)*, *55*(9–10), 1183–1189. https://doi.org/10.1080/0284186X.2016.1182211

Leslie, H. A., van Velzen, M. J. M., Brandsma, S. H., Vethaak, A. D., Garcia-Vallejo, J. J., & Lamoree, M. H. (2022). Discovery and quantification of plastic particle pollution in human blood. *Environment International*, *163*, 107199. https://doi.org/10.1016/J.ENVINT.2022.107199

Li, C., Lau, H. C. H., Zhang, X., & Yu, J. (2022). Mouse Models for Application in Colorectal Cancer: Understanding the Pathogenesis and Relevance to the Human Condition. *Biomedicines*, *10*(7), 1710. https://doi.org/10.3390/BIOMEDICINES10071710

Liang, B., Zhong, Y., Huang, Y., Lin, X., Liu, J., Lin, L., Hu, M., Jiang, J., Dai, M., Wang, B., Zhang, B., Meng, H., Lelaka, J. J. J., Sui, H., Yang, X., & Huang, Z. (2021). Underestimated health risks: polystyrene micro- and nanoplastics jointly induce intestinal barrier dysfunction by ROS-mediated epithelial cell apoptosis. *Particle and Fibre Toxicology*, *18*(1), 20. https://doi.org/10.1186/S12989-021-00414-1

Lichtenstein, P., Holm, N. V., Verkasalo, P. K., Iliadou, A., Kaprio, J., Koskenvuo, M., Pukkala, E., Skytthe, A., & Hemminki, K. (2000). Environmental and heritable factors in the causation of cancer--analyses of cohorts of twins from Sweden, Denmark, and Finland. *The New England Journal of Medicine*, *343*(2), 78–85. https://doi.org/10.1056/NEJM200007133430201

MacLeod, M., Arp, H. P. H., Tekman, M. B., & Jahnke, A. (2021). The global threat from plastic pollution. *Science (New York, N.Y.)*, *373*(6550), 61–65. https://doi.org/10.1126/SCIENCE.ABG5433

Mariano, S., Tacconi, S., Fidaleo, M., Rossi, M., & Dini, L. (2021). Micro and Nanoplastics Identification: Classic Methods and Innovative Detection Techniques. *Frontiers in Toxicology*, *3*, 636640. https://doi.org/10.3389/FTOX.2021.636640/FULL

Moser, A. R., Luongo, C., Gould, K. A., McNeley, M. K., Shoemaker, A. R., & Dove, W. F. (1995). ApcMin: A mouse model for intestinal and mammary tumorigenesis. *European Journal of Cancer*, *31*(7–8), 1061–1064. https://doi.org/10.1016/0959-8049(95)00181-H

Moser, A. R., Pitot, H. C., & Dove, W. F. (1990). A dominant mutation that predisposes to multiple intestinal neoplasia in the mouse. *Science (New York, N.Y.)*, *247*(4940), 322–324. https://doi.org/10.1126/SCIENCE.2296722

Nguyen, L. H., Goel, A., & Chung, D. C. (2020). Pathways of Colorectal Carcinogenesis. *Gastroenterology*, *158*(2), 291–302. https://doi.org/10.1053/j.gastro.2019.08.059

Osman, A. I., Hosny, M., Eltaweil, A. S., Omar, S., Elgarahy, A. M., Farghali, M., Yap, P. S., Wu, Y. S., Nagandran, S., Batumalaie, K., Gopinath, S. C. B., John, O. D., Sekar, M., Saikia, T., Karunanithi, P., Hatta, M. H. M., & Akinyede, K. A. (2023). Microplastic sources, formation, toxicity and remediation: a review. *Environmental Chemistry Letters 2023 21:4*, *21*(4), 2129–2169. https://doi.org/10.1007/S10311-023-01593-3

Perreard, S., B. J., & G. M. (2025). *Plastic Overshoot Day – Report 2025. EA–Earth Action / EA For Impact*. https://plasticovershoot.earth/report-2025/

Prata, J. C. (2018). Airborne microplastics: Consequences to human health? *Environmental Pollution*, *234*, 115–126. https://doi.org/10.1016/j.envpol.2017.11.043

Rawle, D. J., Dumenil, T., Tang, B., Bishop, C. R., Yan, K., Le, T. T., & Suhrbier, A. (2022). Microplastic consumption induces inflammatory signatures in the colon and prolongs a viral arthritis. *Science of the Total Environment*, *809*, *152212*. https://doi.org/10.1016/j.scitotenv.2021.152212

Ren, J., Sui, H., Fang, F., Li, Q., & Li, B. (2019). The application of ApcMin/+ mouse model in colorectal tumor researches. *Journal of Cancer Research and Clinical Oncology*, *145*(5), 1111–1122. https://doi.org/10.1007/S00432-019-02883-6

Rutter, M., Saunders, B., Wilkinson, K., Rumbles, S., Schofield, G., Kamm, M., Williams, C., Price, A., Talbot, I., & Forbes, A. (2004). Severity of Inflammation Is a Risk Factor for Colorectal Neoplasia in Ulcerative Colitis. *Gastroenterology*, *126*(2), 451–459. https://doi.org/10.1053/j.gastro.2003.11.010

Sansom, O. J., Reed, K. R., Hayes, A. J., Ireland, H., Brinkmann, H., Newton, I. P., Batlle, E., Simon-Assmann, P., Clevers, H., Nathke, I. S., Clarke, A. R., & Winton, D. J. (2004). Loss of Apc in vivo immediately perturbs Wnt signaling, differentiation, and migration. *Genes & Development*, *18*(12), 1385–1390. https://doi.org/10.1101/GAD.287404

Schottenfeld, D., Beebe-Dimmer, J. L., & Vigneau, F. D. (2009). The Epidemiology and Pathogenesis of Neoplasia in the Small Intestine. *Annals of Epidemiology*, *19*(1), 58. https://doi.org/10.1016/J.ANNEPIDEM.2008.10.004

Schrock, A. B., Devoe, C. E., McWilliams, R., Sun, J., Aparicio, T., Stephens, P. J., Ross, J. S., Wilson, R., Miller, V. A., Ali, S. M., & Overman, M. J. (2017). Genomic Profiling of Small-Bowel Adenocarcinoma. *JAMA Oncology*, *3*(11), 1546. https://doi.org/10.1001/JAMAONCOL.2017.1051

Sharma, V. K., Ma, X., Lichtfouse, E., & Robert, D. (2022). Nanoplastics are potentially more dangerous than microplastics. *Environmental Chemistry Letters 2022 21:4*, *21*(4), 1933–1936. https://doi.org/10.1007/S10311-022-01539-1

Shepherd, A. L., Smith, A. A. T., Wakelin, K. A., Kuhn, S., Yang, J., Eccles, D. A., & Ronchese, F. (2020). A semi-automated technique for adenoma quantification in the ApcMin mouse using FeatureCounter. *Scientific Reports 2020 10:1*, *10*(1), 3064-. https://doi.org/10.1038/s41598-020-60020-7

Siegel, R. L., Wagle, N. S., Star, J., Kratzer, T. B., Smith, R. A., & Jemal, A. (2026). Colorectal cancer statistics, 2026. *CA: A Cancer Journal for Clinicians*, *76*(2), e70067. https://doi.org/10.3322/CAAC.70067;ISSUE:ISSUE:DOI

Smith, M., Love, D. C., Rochman, C. M., & Neff, R. A. (2018). Microplastics in Seafood and the Implications for Human Health. *Current Environmental Health Reports*, *5*(3), 375. https://doi.org/10.1007/S40572-018-0206-Z

Stock, V., Böhmert, L., Lisicki, E., Block, R., Cara-Carmona, J., Pack, L. K., Selb, R., Lichtenstein, D., Voss, L., Henderson, C. J., Zabinsky, E., Sieg, H., Braeuning, A., & Lampen, A. (2019). Uptake and effects of orally ingested polystyrene microplastic particles in vitro and in vivo. *Archives of Toxicology*, *93*(7), 1817–1833. https://doi.org/10.1007/S00204-019-02478-7

Terzić, J., Grivennikov, S., Karin, E., & Karin, M. (2010). Inflammation and Colon Cancer. *Gastroenterology*, *138*(6), 2101-2114.e5. https://doi.org/10.1053/J.GASTRO.2010.01.058

Van de Wetering, M., Sancho, E., Verweij, C., De Lau, W., Oving, I., Hurlstone, A., Van der Horn, K., Batlle, E., Coudreuse, D., Haramis, A. P., Tjon-Pon-Fong, M., Moerer, P., Van den Born, M., Soete, G., Pals, S., Eilers, M., Medema, R., & Clevers, H. (2002). The β-catenin/TCF-4 complex imposes a crypt progenitor phenotype on colorectal cancer cells. *Cell*, *111*(2), 241–250. https://doi.org/10.1016/S0092-8674(02)01014-0

Walker, T. R., & Fequet, L. (2023). Current trends of unsustainable plastic production and micro(nano)plastic pollution. *TrAC Trends in Analytical Chemistry*, *160*, 116984. https://doi.org/10.1016/J.TRAC.2023.116984

Wang, L., Tu, Y. X., Chen, L., Zhang, Y., Pan, X. L., Yang, S. Q., Zhang, S. J., Li, S. H., Yu, K. C., Song, S., Xu, H. L., Yin, Z. C., Yue, J. Q., Ni, Q. L., Tang, T., Zhang, J. L., Guo, M., Zhang, S., Yao, F., … Chen, Z. X. (2023). Male-Biased Gut Microbiome and Metabolites Aggravate Colorectal Cancer Development. *Advanced Science*, *10*(25), 2206238. https://doi.org/10.1002/ADVS.202206238

Wright, S. L., & Kelly, F. J. (2017). Plastic and Human Health: A Micro Issue? *Environmental Science & Technology*, *51*(12), 6634–6647. https://doi.org/10.1021/ACS.EST.7B00423

Wu, S., Zhang, Y., Lin, Z., & Wei, M. (2025). Global burden of colorectal cancer in 2022 and projections to 2050: incidence and mortality estimates from GLOBOCAN. *BMC Cancer*, *25*(1), 1770. https://doi.org/10.1186/S12885-025-15138-0

Yee, M. S. L., Hii, L. W., Looi, C. K., Lim, W. M., Wong, S. F., Kok, Y. Y., Tan, B. K., Wong, C. Y., & Leong, C. O. (2021). Impact of Microplastics and Nanoplastics on Human Health. *Nanomaterials*, *11*(2), 496. https://doi.org/10.3390/NANO11020496

Yong, C. Q. Y., Valiyaveettil, S., & Tang, B. L. (2020). Toxicity of Microplastics and Nanoplastics in Mammalian Systems. *International Journal of Environmental Research and Public Health*, *17*(5), 1509. https://doi.org/10.3390/IJERPH17051509

Zeng, G., Li, J., Wang, Y., Su, J., Lu, Z., Zhang, F., & Ding, W. (2024). Polystyrene microplastic-induced oxidative stress triggers intestinal barrier dysfunction via the NF-κB/NLRP3/IL-1β/MCLK pathway. *Environmental Pollution*, *345*, *123473*. https://doi.org/10.1016/j.envpol.2024.123473

Zhang, L., & Shay, J. W. (2017). Multiple Roles of APC and its Therapeutic Implications in Colorectal Cancer. *Journal of the National Cancer Institute*, *109*(8), djw332. https://doi.org/10.1093/JNCI/DJW332

Zhang, Z., Chen, W., Chan, H., Peng, J., Zhu, P., Li, J., Jiang, X., Zhang, Z., Wang, Y., Tan, Z., Peng, Y., Zhang, S., Lin, K., & Yung, K. K. L. (2024). Polystyrene microplastics induce size-dependent multi-organ damage in mice: Insights into gut microbiota and fecal metabolites. *Journal of Hazardous Materials*, *461*, *132503*. https://doi.org/10.1016/j.jhazmat.2023.132503

8. Appendix

8.1. Chemical substances and reagents

Supplementary Table 1: PCR compound ratio for one sample

DEPC Treated Water	18 µl
10X PCR Reaction Buffer, Mg 2+ plus	2.5 µl
Primer 1 APC-HindIII fw	1 µl
Primer 2 APC-HindIII rw	1 µl
10 mM dNTP Mix	1 µl
HS Taq DNA Polymerase M101 (5000 U/ml)	0.5 µl
DNA-Extraction template	1 µl
Total	**25 µl**

Supplementary Table 2: HindIII compound ratio for one sample

DEPC Treated Water	4 µl
10x NEBuffer™ r2.1	2 µl
HindIII (20000 U/ml)	2 µl
PCR Product	12 µl
Total	20 µl

Supplementary Table 3: Reagents and solutions used in mouse genotyping

Nr.	Product name	Product-ID	Manufacturer
1	DEPC Treated Water *Pyrogen-free, Nuclease-free*	46-2224	Invitrogen Corp (USA)
2	Proteinase K *(500 mg)*	MCE-HY-108717	MedChemExpress (USA)
3	10X PCR Reaction Buffer, Mg 2+ plus, *10x*	RM20101	ABclonal Technology (USA)
4	Primer 1 APC-HindIII fw *5'-TCTCGTTCTGAGAAAGACAGAAGCT-3'*	4729515	Microsynth AG (Austria)
5	Primer 2 APC-HindIII rw *5'-TGATACTTCTTCCAAAGCTTTGGCTAT-3'*	4729516	Microsynth AG (Austria)

6	dNTP Mix *(10 mM, 1 ml)*	ABM-G129	Applied Biological Materials Inc. (abm) (Canada)
7	HS Taq DNA Polymerase M101 *(5000 U/ml)*	ABC-RK26201-1000U	ABclonal Technology (USA)
8	NEBuffer™ r2.1 *(10x conc.)*	B6002S	New England Biolabs (USA)
9	HindIII (20000 U/ml)	R0104S	New England Biolabs (USA)
10	Quick-Load® Purple 100 bp DNA Ladder	N0551G	New England Biolabs (USA)
11	DNA Loading Dye 6x	ABM-G030	New England Biolabs (USA)
12	Midori Green Advance	MG 04	NIPPON Genetics EUROPE GmbH (Germany)
13	Hoechst 33342 (trihydrochloride) *50mg*	MCE-HY-15559A-50MG	MedChemExpress (USA)
14	Dextran sulfate sodium salt, colitis grade	9011-18-1	MP Biomedicals (USA, Germany)
15	0.5 M EDTA, pH 8	15575-038	Invitrogen Corp (USA)
16	Physiological saline solution for infusion „Fresenius"	1-16417	Fresenius Kabi Austria GmbH (Austria)
17	Ketasol *100 mg/ml*		Livisto (Germany)
18	Xylasol *20 mg/ml*		Livisto (Germany)

Supplementary Table 4: Routinely used chemical solutions and substances

Nr.	Product name	Product-ID	Manufacturer
1	2-Propanol *(min. 99.5 %)*	CP41.2	Carl Roth GmbH+Co (Germany)
2	Mayer's hemalum solution	1.09249.0500	Sigma-Aldrich (Germany)
3	SCOTTsche-Lösung	11192.01000	MORPHISTO GmbH (Germany)
4	Eosin 1%, aqueous	10177.01000	MORPHISTO GmbH (Germany)
5	Acetic acid *(≥95%)*	A6283-500ML	Honeywell (Germany)
6	Xylene *(99%)*	1330-20-7	ThermoFisher scientific (Belgium, UK)
7	n-Butyl acetate	1.09652.2500	Sigma-Aldrich (Germany)
8	Ethanol absolute	20821.310	VWR International GmbH (France)

9	Eukitt® mounting medium	03989-100ML	VWR International GmbH (France)
10	Methanol *(99.8%)*	67-56-1	ThermoFisher scientific (Belgium, UK)
11	Formaldehyde solution 4,5%, *buffered, neutral*	FN-1000-45-1	SAV Liquid Production GmbH (Germany)
12	Sodium chloride	1.06404.1000	Sigma-Aldrich (Germany)
13	Agarose	A9539-250G	Sigma-Aldrich (Germany)
14	SDS (Sodium Dodecyl Sulfate)	161-0302	Bio-Rad Laboratories (USA)
15	Tris(hydroxymethyl)aminomethane	1.08382.1000	Sigma-Aldrich (Germany)
16	Sodium dihydrogen phosphate monohydrate	1.06346.0500	Merck Millipore (USA)
17	di-Sodium hydrogen phosphate dihydrate	1.06580.1000	Merck Millipore (USA
18	Tween 20	170-6531	Bio-Rad Laboratories (USA)

Supplementary Table 5: Routinely used laboratory equipment and consumables

Nr.	Product name	Product-ID	Manufacturer
1	Cover slips *(square and rectangular, 24 x 50 mm)*	1871.2	Carl Roth GmbH+Co (Germany)
2	Microscope slides Superfrost Plus *(25 mm x 75 mm x 1mm)*	H867.1	Carl Roth GmbH+Co (Germany)
3	Permanent aqueous mounting medium	OOSA09601-30ML	Aviva Systems Biology (USA)
4	Paraffin (Histo-Comp) *2 kg*	VO-5-1001	Vogel MedTec GmbH (Germany)
5	Tissue embedding cassettes	053748 053723	KABE LABORTECHNIK GmbH
6	Towerpack Pipetman Diamond Tips - Pipette Tips	F167104 F167103 F167102	Gilson S.A.S (France)
7	Safe-Lock Tubes *1.5 ml*	0030120086	Eppendorf SE (Germany)
8	PCR Tube Strips *0.2 ml*	951010022	Eppendorf SE (Germany)
9	Injekt® Luer Solo *20 ml*	4606205V	B. Braun SE (Germany)
10	Sterile single use stainless surgical blades *Size 10, No 3*	L.301	Lance Paragon LTD. (UK)
11	MiniCollect® Tube *1 ml* K3E K3EDTA	450531	Greiner Bio-One GmbH (Austria)
12	Tuberculin syringe 1 *ml*	CHTUB01	CHIRANA T. Injecta (Slovakia)
13	Sterican® standard needles, *0.60 x 30 mm*	4657640B	B. Braun SE (Germany)

Supplementary Table 6: Formulation of the Lysis buffer for mouse DNA extraction.

Compound	per 500 ml
1 M TRIS pH 8.0	50 ml
0.2 M EDTA pH 8.0	12.5 ml
4 M NaCl	25 ml
10% SDS	5 ml
dH_2O	fill to 500 ml

Supplementary Table 7: Formulation of a 50x TAE buffer stock solution. Needs to be diluted 1:50 with purified water in order to create a 1x TAE buffer solution.

Compound	Per 1000 ml
TRIS	242.3 g
Glacial acetic acid	57.2 ml
0.5 M EDTA (pH 8.0)	100 ml
Purified water	ad 1000 ml

Supplementary Table 8: Laboratory equipment used for genotyping and sample processing.

Nr.	Device	Manufacturer	Picture
1	C1000 Touch Thermal Cycler	Bio-Rad Laboratories (USA)	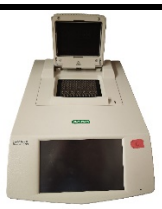
2	PowerPac™ Basic Power Supply	Bio-Rad Laboratories (USA)	
3	Axio Imager M2	Carl Zeiss AG (Germany)	
4	ChemiDoc MP Imaging System	Bio-Rad Laboratories (USA)	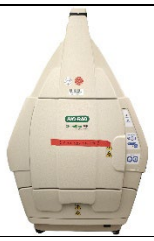

12	Tissue-Tek® TEC™ 6 Embedding Module	Sakura Finetek (Japan)	
13	Microm HM 340E	ThermoFisher scientific (Belgium, UK)	

8.2.Mouse food preparation

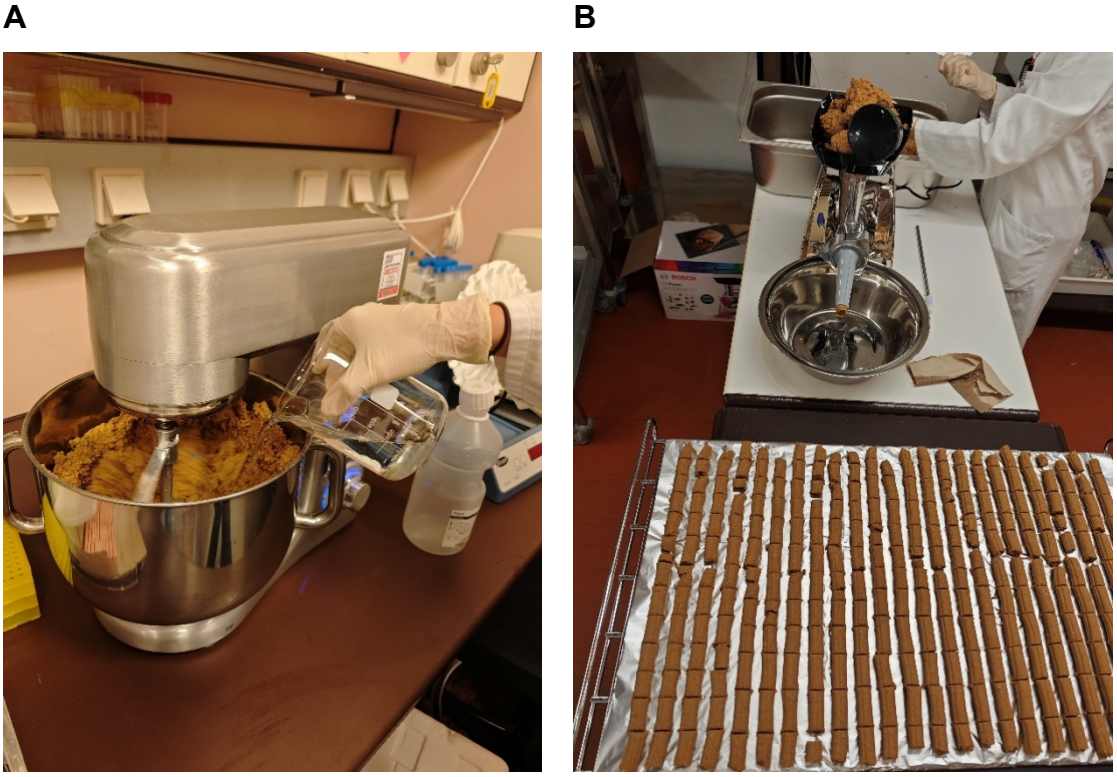

Supplementary Figure 1: MNP mouse food preparation. MNP-water mixture gradually added to homogenised mouse food (A). Forming of mouse food pellets (B).

8.3. Paraffin embedding and cutting

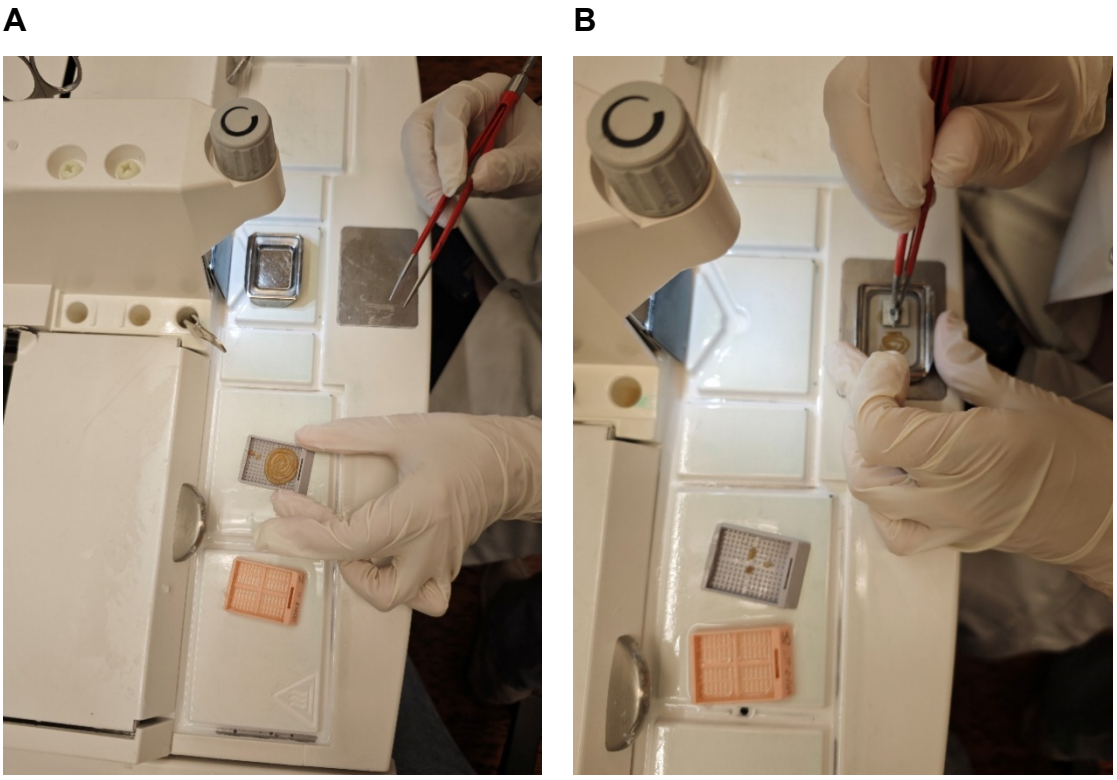

Supplementary Figure 2: Small intestine embedding in paraffin. Warming up of paraffin-infused histological cassettes in order to retrieve and transfer the organ (A). After adequate organ placement in mold and submergence with paraffin the organs had to be held down and cooled.

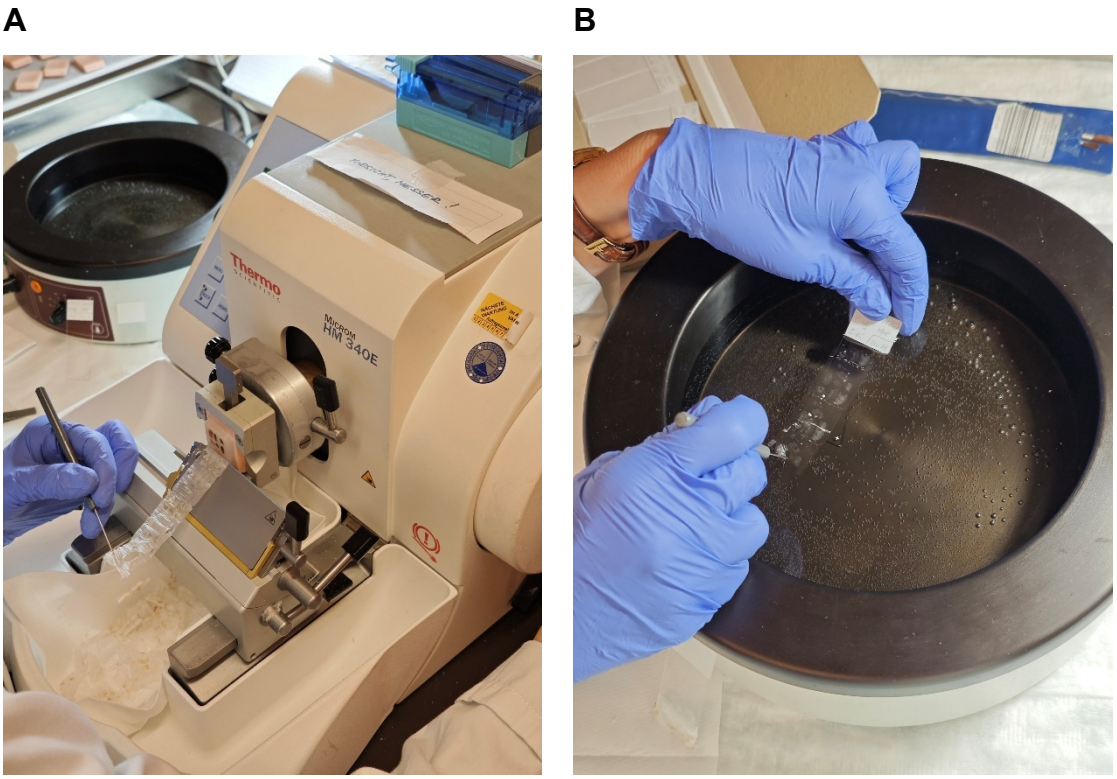

Supplementary Figure 3. Paraffin-embedded tissue section preparation using a microtome. Samples were cut in long bands at a thickness of 3 µm (A). Sections floating in a waterbath for stretching and being mounted on a glass slide (B).

8.4. Antibodies and blocking solutions for immunohistochemical staining

Supplementary Table 9: List of antibodies and reagents for immunohistochemical staining.

Nr.	Product name	Product-ID	Concentration	Buffer	Manufacturer
1	Arginase-1 XP® Rabbit mAb	93668	1:120	Citrate buffer pH6	Cell Signalling Technology (USA)
2	iNOS Rabbit mAb	68186	1:1000	Citrate buffer pH6	Cell Signalling Technology (USA)
3	F4/80 XP® Rabbit mAb	70076	1:150	Citrate buffer pH6	Cell Signalling Technology (USA)
4	Neutrophil Elastase Rabbit mAb	90120	1:150	TRIS-EDTA buffer pH9	Cell Signalling Technology (USA)
5	Mouse/Rabbit ImmunoDetector DAB HRP Brown	BSB-0004	-	-	Bio SB (USA)
6	Tris-EDTA HIER Solution (10x) pH9	NB-TES500	-	-	THP Medical Products Vertriebs GmbH (Austria)
7	Superblock	NB-AAA125	-	-	THP Medical Products Vertriebs GmbH (Austria)
8	Mouse-to-Mouse Blocking Reagent	NB-MTM125	-	-	THP Medical Products Vertriebs GmbH (Austria)